Available online at www.sciencedirect.com
SCIENCE DIRECT®
Analytical Biochemistry 326 (2004) 262–266
ANALYTICAL BIOCHEMISTRY
www.elsevier.com/locate/yabio

Microanalysis for MDR1 ATPase by high-performance liquid chromatography with a titanium dioxide column

Yasuhisa Kimura,[a] Seiji Shibasaki,[b,c,1] Kei Morisato,[d] Norio Ishizuka,[d] Hiroyoshi Minakuchi,[d] Kazuki Nakanishi,[e] Michinori Matsuo,[a] Teruo Amachi,[a] Mitsuyoshi Ueda,[c] and Kazumitsu Ueda[a,*]

[a] *Division of Applied Life Sciences, Graduate School of Agriculture, Kyoto University, Kyoto 606-8502, Japan*
[b] *Department of Applied Chemistry, Kobe City College of Technology, Gakuen-higashimachi, Nishiku, Kobe 651-2194, Japan*
[c] *Department of Synthetic Chemistry and Biological Chemistry, Graduate School of Engineering, Kyoto University, Yoshida, Sakyo-ku, Kyoto 606-8501, Japan*
[d] *Kyoto Monotech, Shibanomiya-cho, Shimotsubayashi, Nishikyo-ku, Kyoto 615-8053, Japan*
[e] *Department of Material Chemistry, Graduate School of Engineering, Kyoto University, Kyoto 606, Japan*

Received 9 October 2003

Abstract

MDR1 is clinically important because it is involved in multidrug resistance of cancer cells and affects the pharmacokinetics of various drugs. Because MDR1 harnesses adenosine 5′-triphosphate (ATP) hydrolysis for transporting drugs, examining the effect on ATPase activity is imperative for understanding the interactions between drugs and MDR1. However, conventional assay systems for ATPase activity are not sensitive enough for screening drugs using purified MDR1. Here we report a novel method to measure ATPase activity of MDR1 using high-performance liquid chromatography equipped with a titanium dioxide column. The amount of adenosine 5′-diphosphate (ADP) produced by the ATPase reaction was determined within 2 min with a titanium dioxide column (4.6 mm ID × 100 mm). The relationship between ADP amount and chromatogram peak area was linear from 5 pmol to 10 nmol. This method made it possible to reduce the amount of purified MDR1 required for a reaction to 0.5 ng, about 1/20th of the conventional colorimetric inorganic phosphate detection assay. This method is sensitive enough to detect any subtle changes in ATPase activity of MDR1 induced by drugs and can be applied to measure ATPase activity of any protein.

Keywords: MDR1; ATPase; Titanium dioxide column

MDR1 is a plasma membrane-located protein that confers multidrug resistance to mammalian cells by actively transporting various compounds out of cells. MDR1 is clinically important not only because it is involved in multidrug resistance of cancer cells [1,2] but also because it affects the pharmacokinetics of various drugs [3]. MDR1 in the mucosal epithelium of intestinal cells is a major limiting factor for the rate of uptake of some drugs from the intestinal lumen [4–6]. Screening of drugs that are not transported by MDR1 is important for developing drugs of high oral availability. Because drug transport by MDR1 is dependent on ATP hydrolysis and because most substrates transported by MDR1 stimulate ATP hydrolysis, examining the effect on ATPase activity is imperative for understanding the interaction between drugs and MDR1. However, no reliable and convenient screening system based on ATPase activity of human MDR1 has been developed yet.

The commonly used method to measure ATPase activity is the spectrometric measurement of phosphomolybdate complexes formed by the reaction between ammonium molybdate and inorganic phosphate released from ATP (Pi-Mo method) [7]. However, the Pi-Mo method is not sensitive enough to measure low ATPase activity, especially if a large amount of purified enzyme is not available. Luciferase assay is

* Corresponding author. Fax: +81-75-753-6104.
E-mail address: uedak@kais.kyoto-u.ac.jp (K. Ueda).
[1] This author contributed to this work equally with the first author.

0003-2697/$ - see front matter © 2004 Elsevier Inc. All rights reserved.
doi:10.1016/j.ab.2003.12.012

highly sensitive to quantify ATP, but it cannot be used to measure low ATPase activity at physiological concentrations (2–3 mM) of ATP. Reversed-phase high-performance liquid chromatography (HPLC) has been reported as a highly sensitive method to measure amounts of ATP and ADP with linearity over a wide range from 0.05 to 10 nmol [8]. However, because these methods take 10 to 15 min for one assay, it may not be applicable for high-throughput screening [8–10]. Determination of radioactive phosphate from [^{32}P]ATP is sensitive, but this method needs extra radioisotope facilities.

TiO_2 selectively adsorbs organic phosphates, as reported by Matsuda et al. [11], and can be used to separate adenine nucleotides. We applied HPLC equipped with a titanium dioxide column for measuring ATPase activity of human MDR1. This column greatly improved the sensitivity and reduced the time required for each assay.

Materials and methods

Materials

Sf9 cells were purchased from Pharmingen. L-α-lecithin, ATP, ADP, AMP, and adenosine were from Sigma–Aldrich. Media, pluronic F-68, and gentamycin were obtained from Invitrogen. *N*-dodecyl-β-D-maltoside (DDM) was purchased from Anatrace. Sodium ortho-vanadate and verapamil hydrochloride were purchased from Wako.

Generation of recombinant baculovirus encoding His × 10 tagged MDR1

The sequence encoding thrombin cleavage site, 10 histidine codons, and a termination codon were inserted at the 3′ end of human *MDR1* cDNA [12]. The modified *MDR1* cDNA (MDR1-TH) was subcloned into the transfer vector pVL1392 (Pharmingen). Recombinant baculovirus encoding MDR1-TH (BV-MDR1-TH) was generated by cotransfection of Sf9 cells with pVL1392-MDR1-TH and Baculogold DNA (Pharmingen). BV-MDR1-TH was purified and amplified according to the manufacturer's protocol. Virus titer was determined by plaque assay.

Protein expression and preparation of microsomes

Sf9 cells were cultured in 7:3 mixture of IPL41 and Sf900II media. To avoid cell aggregation and contamination of microorganisms, pluronic F-68 and gentamycin were added at final concentrations of 0.1% and 10 μg/ml, respectively. Sf9 cells were infected with BV-MDR1-TH at a multiplicity of infection 5. After 48 h incubation, cells were harvested and washed with five-volumes of ice-cold phosphate-buffered saline. The cell pellet was stored at −80 °C. Frozen Sf9 cells were resuspended in 10-fold volume of sonication buffer (20 mM Tris–Cl, pH 7.5, 10% v/v glycerol, 1 mM EDTA). All further steps were done at 4 °C or on ice. Cells were disrupted by Ultrasonic processor XL (Misonix) for 30 s at output level 5 and then returned to the ice for 2 min. These steps were repeated 10 times. The suspension was centrifuged at 650*g* for 10 min. The pellet (unbroken cells) was sonicated again as above and centrifuged, and the pellet was discarded. The homogenate was centrifuged at 2000*g* for 30 min to remove nuclei. The supernatant was centrifuged at 40,000*g* for 60 min. The pellet containing the microsomes was resuspended in ice-cold buffer A (50 mM Tris–Cl, pH 8.0, 50 mM NaCl, 30% v/v glycerol 15 mM imidazole, 1 mM 2-mercaptoethanol) containing protease inhibitors as follows: 100 μg/ml *p*-amidinophenylmethylsulfonyl fluoride, 10 μg/ml leupeptin, 2 μg/ml aprotinin. The microsomes were stored at −80 °C.

Purification of MDR1

Microsomes were thawed on ice and diluted to 4 mg protein/ml with ice-cold buffer A plus protease inhibitors. An equal volume of 1.2% w/v DDM in buffer A plus protease inhibitor was added to the solution, and the suspension was mixed by inversion and kept on ice for 10 min. Insoluble proteins were removed by centrifugation (60,000*g*, 30 min). Then, nickel-nitrilotriacetate agarose resin (Qiagen) was added to the supernatant at a ratio of 0.5 ml of resin per 100 mg of solubilized microsomal protein. MDR1 can be purified with this resin because of a strong interaction of nickel-nitrilotriacetate with tandem histidine side chains fused to the carboxyl terminus of MDR1. The slurry was incubated at 4 °C for 18 h with continuous rotation. The resin was washed with a 10-bed volume of buffer A containing 0.1% DDM three times and then with five volumes of buffer A containing 0.1% DDM plus 40 mM imidazole. MDR1 was eluted with five volumes of buffer A containing 0.1% DDM plus 300 mM imidazole. Protein concentration was estimated by the Bradford method (Bio-Rad).

ATP hydrolysis reaction

For lipid stocks, L-α-lecithin was solubilized in 40 mM Tris–Cl, pH 7.5, 0.1 mM EGTA at a concentration of 20 mg/ml by sonicating in a bath sonicator (Bioruptor CD-200 TM; COSMO BIO) until the suspension clarified. Lipid stocks were stored at 4 °C. Purified MDR1 and lipid stocks were mixed at protein/lipid ratio at 1/5 (w/w) in 40 mM Tris–Cl, pH 7.5, 0.1 mM EGTA, 2 mM dithiothreitol at 23 °C for 20 min and then sonicated at 4 °C for 30 s in a bath sonicator. Reconstituted protein was reacted in 15 μl of 40 mM

Tris–Cl (pH 7.5), 0.1 mM EGTA, 1 mM NaATP, 1 mM $MgCl_2$ and 0.1 mM verapamil in the presence or absence of 0.4 mM ortho-vanadate and 0.1 mM beryllium fluoride at 37 °C for 30 min. The reaction was stopped by heating the reaction mixture at 100 °C for 5 s by thermal cycler PTC-200 (MJ-Reserch) in the case of HPLC detection and by adding an equal volume of 12% SDS in the case of colorimetric detection. MDR1 completely lost its ATPase activity with these treatments. For HPLC detection, 5 µl of heat-inactivated sample was analyzed.

HPLC apparatus and chromatographic conditions

The liquid chromatographic equipment consisted of an LC-10ADVP pump and an SPD-M10AVP diode array detector (Shimadzu). Data were recorded and analyzed with a CLASS-VP software system Version 5.03 (Shimadzu). The detection wavelength was set at 260 nm. ATP and ADP were separated on a Titansphere TiO column (4.6 mm ID × 100 mm; GL Sciences). Chromatographic determination was performed at 40 °C and at a 2 ml/min flow rate. The mobile phase was composed of NaH_2PO_4 buffer (50 mM, pH 7) and 50% v/v acetonitrile (Wako).

Colorimetric detection

The colorimetric detection was done as described previously [7]. After the reaction was stopped by SDS, 10 µl of H_2O was added on sample. Color development started with the addition of 40 µl of equal mixture of 1% ammonium molybdate and 6% ascorbic acid in 1 N HCl. After 7 min incubation at room temperature, 60 µl of 2% sodium citrate, 2% sodium arsenite, 2% acetic acid were added and incubated at 37 °C for 10 min. The color absorbance was measured at 850 nm by UV–VIS spectrophotometer UV mini 1240 (Shimadzu).

Results

Nucleotide separation with a titanium dioxide column

It has been reported [8] that ATP and ADP can be separated with a reversed-phase HPLC column with linearity over a wide range from 0.05 to 10 nmol. However, because the method with a reversed-phase HPLC column takes about 10–15 min for one assay [8–10], it may not be applicable for high-throughput screening. Therefore, we tried to use a titanium dioxide column. A chromatogram of nucleotides is shown in Fig. 1A. Adenosine, AMP, ADP, and ATP were separated within 3 min, and the retention time of each compound was 0.62, 0.92, 1.39, and 2.37 min, respectively. The relationship between ADP amount and chromatogram peak area was linear from 5 pmol to 10 nmol with a coefficient of determination (r^2) of 1.00 as shown in Fig. 1B.

Measurement of ATPase activity of purified MDR1 with a titanium dioxide column

Human MDR1 was successfully expressed in high levels in insect cells with a MDR1 recombinant baculovirus. Immunoblot analysis suggested that most of

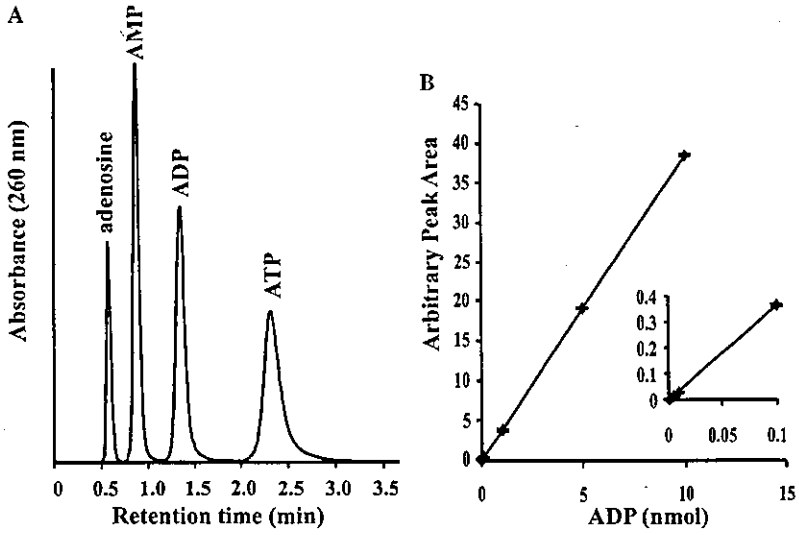

Fig. 1. Nucleotide separation by a titanium dioxide column and relationship between chromatogram peak area and amount of ADP. (A) Separation of nucleotide. The mixture of nucleotide (adenosine, 5 nmol; AMP, ADP, ATP, 10 nmol) was injected to titanium dioxide column (4.6 mm ID × 100 mm) at 0 min. Separation was carried by 50 mM Na-Pi buffer (pH 7.0), 50% v/v acetonitrile at 40 °C. Absorbance at 260 nm was recorded. Adenosine, AMP, ADP, and ATP were eluted at 0.62, 0.92, 1.39, and 2.37 min, respectively. (B) Relationship between peak area and amount of ADP. The inset shows a relationship at low concentrations of ADP. The straight line was drawn by linear regression. Experiments were done in duplicate.

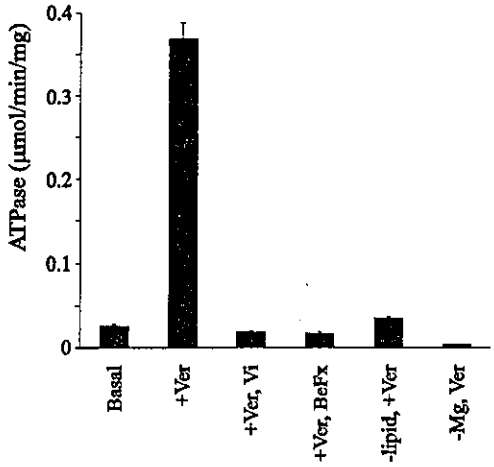

Fig. 2. Characteristics of ATPase activity of the purified MDR1. The purified MDR1 (100 ng) was reconstituted in liposome as described under Materials and methods. Reactions were done in the absence or in the presence of 0.1 mM verapamil (Ver), 0.4 mM ortho-vanadate (Vi), and 0.1 mM beryllium fluoride (BeFx). ATPase activity was estimated by quantifying the released ADP by HPLC analysis. Standard deviations ($N = 3$) are shown by bars.

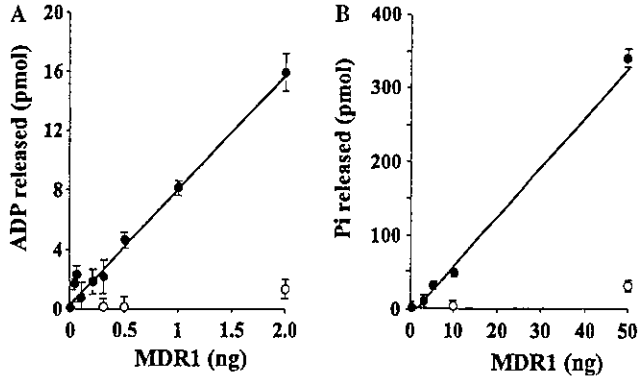

Fig. 3. Relation between released ADP and amount of the purified MDR1. (A) Amount of released ADP measured by the HPLC method. (B) Amount of inorganic phosphate measured by the Pi-Mo method. Reaction was done in the presence (●) or in the absence (○) of 100 μM verapamil. The coefficients of determination (r^2) were 0.977 (A) and 0.971 (B), respectively. The straight line was drawn by linear regression. Standard deviations ($N = 3$) are shown by bars.

MDR1 in a membrane fraction was solubilized by 0.6% DDM and bound to nickel-nitrilotriacetate agarose resin (data not shown). As an eluate of 300 mM imidazole solution, more than 95% purity of human MDR1 was obtained by single-step purification (data not shown) as reported previously for MDR1 expressed in yeasts and mammalian cells [13–15]. Membrane proteins (350 mg) were obtained from 15 g of Sf9 cells grown in 1 L culture, and about 3.5 mg of the purified MDR1 protein was extracted from DDM-solubilized membrane.

ATPase activity of the purified MDR1 was measured by HPLC equipped with a titanium dioxide column. The purified protein showed the typical ATPase activity of MDR1 (Fig. 2) as reported [13,14,16–18]: (i) low basal activity, (ii) strong stimulation by verapamil, (iii) dependence on Mg^{2+}, and (iv) complete inhibition by phosphate analogs ortho-vanadate (Vi) and beryllium fluoride (BeFx). Verapamil-induced ATPase activity was hardly detected without reconstitution to a liposome, suggesting that the lipid environment is quite important for the function of MDR1 as reported before [19]. The K_m for ATP of verapamil-stimulated ATPase activity of purified MDR1 was 0.3 mM (data not shown), also in good agreement with previously reported K_m values for MDR1.

Sensitivity of titanium dioxide column method to drug-stimulated ATPase activity

Because ADP, as low as 5 pmol, can be detected with titanium dioxide column method (Fig. 1B), this new method is expected to be much more sensitive in measuring ATPase acitivity than conventional methods. We examined the sensitivity of this method to measure drug-stimulated ATPase activity of purified MDR1 and compared it to the Pi-Mo method. The relationships between the amount of the purified MDR1 and the released ADP measured by these methods were both linear with coefficients of determination (r^2) of 0.977 (Fig. 3A) and 0.971 (Fig. 3B), respectively. The drug-stimulated ATPase activity of MDR1 was clearly detected with 0.5 ng of the purified protein with the titanium dioxide column method; however, at least 10 ng was required with the Pi-Mo method.

Discussion

In this report, we describe a novel method for measuring the ATPase activity of human MDR1 using purified protein and HPLC equipped with a titanium dioxide column. This method is highly sensitive and able to detect subtle changes in ATPase activity of MDR1 induced by drugs and is suitable for automated high-throughput screening.

Application of HPLC equipped with a titanium dioxide column in measuring ADP made it possible to reduce the amount of the purified MDR1 required for the reaction to 1/20th of the amount used in conventional colorimetric inorganic phosphate detection assays [7]. From a 1-L culture of Sf9 cells, 3.5 mg of the purified human MDR1 can be obtained, allowing more than 3 million reactions to occur. Furthermore, the titanium dioxide column showed good separation of nucleotides in much less elution time compared to the reversed-phase HPLC analyses previously reported [8–10].

Measuring ATPase activity using the purified MDR1 has several advantages. This assay system shows very low basal ATPase activity and is suitable for detecting stimulation of MDR1 ATPase. This assay system does

not include any inhibitors to repress other endogenous membrane ATPase unlike other assay systems, such as using microsomes from Sf9 insect cells expressing human MDR1 [20,21]. The direct effects of drugs on MDR1 ATPase can be measured by this method, making the interpretation of results much simpler.

MDR1 is an important target for developing drugs, not only because it is involved in multidrug resistance of tumor cells but also because it may be involved in tumorigenesis as reported recently [22,23]. The effective screening system, reported here, for drugs interacting with MDR1 may facilitate the development of new chemotherapeutic drugs for preventing multidrug resistance and tumorigenesis and for developing drugs of high oral availability.

Acknowledgments

We thank Ikuma Kuroda, Syota Miyazaki, and Masahiro Furuno (GL Sciences Co. Ltd.) for excellent technical assistance. This work was supported by research grants from the Ministry of Education, Science, Sports, and Culture of Japan and the Bio-oriented Technology Research Advancement Institution.

References

[1] R.L. Juliano, V. Ling, A surface glycoprotein modulating drug permeability in Chinese hamster ovary cell mutants, Biochim. Biophys. Acta 455 (1976) 152–162.

[2] K. Ueda, C. Cardarelli, M.M. Gottesman, I. Pastan, Expression of a full-length cDNA for the human MDR1 gene confers resistance to colchicine, doxorubicin, and vinblastine, Proc. Natl. Acad. Sci. USA 84 (1987) 3004–3008.

[3] K. Westphal, A. Weinbrenner, M. Zschiesche, G. Franke, M. Knoke, R. Oertel, P. Fritz, O. von Richter, R. Warzok, T. Hachenberg, H.M. Kauffmann, D. Schrenk, B. Terhaag, H.K. Kroemer, W. Siegmund, Induction of P-glycoprotein by rifampin increases intestinal secretion of talinolol in human beings: a new type of drug/drug interaction, Clin. Pharmacol. Ther. 68 (2000) 345–355.

[4] S.V. Ambudkar, S. Dey, C.A. Hrycyna, M. Ramachandra, I. Pastan, M.M. Gottesman, Biochemical, cellular, and pharmacological aspects of the multidrug transporter, Annu. Rev. Pharmacol. Toxicol. 39 (1999) 361–398.

[5] B. Greiner, M. Eichelbaum, P. Fritz, H.P. Kreichgauer, O. von Richter, J. Zundler, H.K. Kroemer, The role of intestinal P-glycoprotein in the interaction of digoxin and rifampin, J. Clin. Invest. 104 (1999) 147–153.

[6] H. Suzuki, Y. Sugiyama, Role of metabolic enzymes and efflux transporters in the absorption of drugs from the small intestine, Eur. J. Pharm. Sci. 12 (2000) 3–12.

[7] S. Chifflet, A. Torriglia, R. Chiesa, S. Tolosa, A method for the determination of inorganic phosphate in the presence of labile organic phosphate and high concentrations of protein: application to lens ATPases, Anal. Biochem. 168 (1988) 1–4.

[8] K. Samizo, R. Ishikawa, A. Nakamura, K. Kohama, A highly sensitive method for measurement of myosin ATPase activity by reversed-phase high-performance liquid chromatography, Anal. Biochem. 293 (2001) 212–215.

[9] J. Sudo, J. Terui, H. Iwase, K. Kakuno, Assay of ATPase and Na,K-ATPase activity using high-performance liquid chromatographic determination of ADP derived from ATP, J. Chromatogr. B. Biomed. Sci. Appl. 744 (2000) 19–23.

[10] M. Ushimaru, Y. Fukushima, Complete separation of adenine nucleotides for ATPase activity assay by ion-pair reversed-phase high-performance liquid chromatography, Anal. Biochem. 313 (2003) 173–175.

[11] H. Matsuda, H. Nakamura, T. Nakajima, New ceramic titania: selective adsorbent for organic phosphates, Anal. Sci. 6 (1990) 911–912.

[12] N. Kioka, J. Tsubota, Y. Kakehi, T. Komano, M.M. Gottesman, I. Pastan, K. Ueda, P-glycoprotein gene (MDR1) cDNA from human adrenal: normal P-glycoprotein carries Gly185 with an altered pattern of multidrug resistance, Biochem. Biophys. Res. Commun. 162 (1989) 224–231.

[13] N. Lerner-Marmarosh, K. Gimi, I.L. Urbatsch, P. Gros, A.E. Senior, Large scale purification of detergent-soluble P-glycoprotein from Pichia pastoris cells and characterization of nucleotide binding properties of wild-type, Walker A, and Walker B mutant proteins, J. Biol. Chem. 274 (1999) 34711–34718.

[14] Q. Mao, G.A. Scarborough, Purification of functional human P-glycoprotein expressed in *Saccharomyces cerevisiae*, Biochim. Biophys. Acta 5 (1997) 107–118.

[15] T.W. Loo, D.M. Clarke, Rapid purification of human P-glycoprotein mutants expressed transiently in HEK 293 cells by nickel-chelate chromatography and characterization of their drug-stimulated ATPase activities, J. Biol. Chem. 270 (1995) 21449–21452.

[16] F.J. Sharom, X. Yu, C.A. Doige, Functional reconstitution of drug transport and ATPase activity in proteoliposomes containing partially purified P-glycoprotein, J. Biol. Chem. 268 (1993) 24197–24202.

[17] S.V. Ambudkar, Purification and reconstitution of functional human P-glycoprotein, J. Bioenerg. Biomembr. 27 (1995) 23–29.

[18] I.L. Urbatsch, M.K. al-Shawi, A.E. Senior, Characterization of the ATPase activity of purified Chinese hamster P-glycoprotein, Biochemistry 33 (1994) 7069–7076.

[19] A. Rothnie, D. Theron, L. Soceneantu, C. Martin, M. Traikia, G. Berridge, C.F. Higgins, P.F. Devaux, R. Callaghan, The importance of cholesterol in maintenance of P-glycoprotein activity and its membrane perturbing influence, Eur. Biophys. J. 30 (2001) 430–442.

[20] B. Sarkadi, E.M. Price, R.C. Boucher, U.A. Germann, G.A. Scarborough, Expression of the human multidrug resistance cDNA in insect cells generates a high activity drug-stimulated membrane ATPase, J. Biol. Chem. 267 (1992) 4854–4858.

[21] G.A. Scarborough, Drug-stimulated ATPase activity of the human P-glycoprotein, J. Bioenerg. Biomembr. 27 (1995) 37–41.

[22] Y. Mochida, K. Taguchi, S. Taniguchi, M. Tsuneyoshi, H. Kuwano, T. Tsuzuki, M. Kuwano, M. Wada, The role of P-glycoprotein in intestinal tumorigenesis: disruption of mdr1a suppresses polyp formation in Apc(Min/+) mice, Carcinogenesis 24 (2003) 1219–1224.

[23] T. Yamada, Y. Mori, R. Hayashi, M. Takada, Y. Ino, Y. Naishiro, T. Kondo, S. Hirohashi, Suppression of intestinal polyposis in Mdr1-deficient ApcMin/+ mice, Cancer Res. 63 (2003) 895–901.

ATP Hydrolysis-Dependent Multidrug Efflux Transporter: MDR1/P-glycoprotein

Yasuhisa Kimura[1], Michinori Matsuo[1], Kei Takahashi[1], Tohru Saeki[2], Noriyuki Kioka[1], Teruo Amachi[1] and Kazumitsu Ueda[1,*]

[1]*Laboratory of Cellular Biochemistry, Division of Applied Life Sciences, Graduate School of Agriculture, Kyoto University, Kyoto 606-8502;* [2]*Laboratory of Molecular Nutrition, Department of Biological Function, Graduate School of Agriculture Kyoto Prefectural University, Kyoto 606-8522, Japan.*

Abstract: P-glycoprotein/MDR1 was the first member of the ATP-binding cassette (ABC) transporter superfamily to be identified in a eukaryote. In eukaryotes, ABC proteins can be classified into three major groups based on function: transporters, regulators, and channels. MDR1/P-glycoprotein is a prominent member of eukaryotic export-type ABC proteins. MDR1/P-glycoprotein extrudes a very wide array of structurally dissimilar compounds, all lipophilic and ranging in mass from approximately 300 to 2000 Da, including cytotoxic drugs that act on different intracellular targets, steroid hormones, peptide antibiotics, immunosuppressive agents, calcium channel blockers, and others. Nucleotide binding and hydrolysis by MDR1/P-glycorptrotein is tightly coupled with its function, substrate transport. ATP binding and hydrolysis were extensively analyzed with the purified MDR1/P-glycoprotein. The vanadate-induced nucleotide trapping method was also applied to study the hydrolysis of ATP by MDR1/P-glycoprotein. When MDR1 hydrolyzes ATP in the presence of excess orthovanadate, an analog of inorganic phosphate, it forms a metastable complex after hydrolysis. Using this method, MDR1/P-glycoprotein can be specifically photoaffinity-labeled in the membrane, if 8-azido-[α^{32}P]ATP is used as ATP. Visualization of the structure, as well as the biochemical data, is needed to fully understand how MDR1/P-glycoprotein recognizes such a variety of compounds and how it carries its substrates across the membrane using the energy from ATP hydrolysis. To do so, large amounts of pure and stable proteins are required. Heterologous expression systems, which have been used to express P-glycoprotein, are also described.

INTRODUCTION

P-glycoprotein/MDR1 was the first member of the ATP-binding cassette (ABC) transporter superfamily to be identified in a eukaryote. P-glycoprotein was originally recognized as a surface glycoprotein, which was overexpressed in drug-resistant Chinese hamster ovary cell mutants [1]. Levels of multi-drug resistance of these Chinese hamster cells [2] and human multidrug resistant KB carcinoma cell lines [3] were shown to correlate with the amplification of specific DNA segments. Human MDR1 cDNA was isolated from a multidrug resistant KB cell line, KB-C2.5, selected for resistance to colchicine in 1986 [4,5] and turned out to code for P-glycoprotein [6]. Around the same time, mouse mdr1 cDNA was isolated by Gros *et al.* [7]. The cDNA segment encoding Chinese hamster P-glycoprotein was isolated by using a monoclonal antibody [8]. Afterwards, the human MDR1 cDNA isolated from KB-C2.5 was found to be associated with a Gly-to-Val substitution at position 185, in the predicted cytoplasmic loop between TM2 and TM3. This mutation, which increased colchicine resistance and decreased vinblastine resistance, occurred in the course of extensive colchicine selection [9]. The human MDR1 cDNA from normal tissue was isolated in 1989. It contained Gly at position 185 and genetic polymorphism at codon 893 [10]. The amino acid sequence of the MDR1 P-glycoprotein, deduced from its nucleotide sequence, shares homology with potential nucleotide binding sites of peripheral membrane components of bacterial active transporter systems [4,7]. We suspected that MDR1 by itself could function as an energy-dependent efflux pump responsible for decreased drug accumulation in multidrug-resistant cancer cells [4]. Indeed, the overexpression of human and mouse MDR1/P-glycoprotein conferred resistance to multiple drugs such as *Vinca* alkaloids, anthracyclines, epipodophyllotoxins, and taxol [5,11,12]. Tumors arising from tissues where MDR1/P-glycoprotein is highly expressed show intrinsic resistance to chemotherapy, while acquired resistance is often correlated with an increased expression of MDR1/P-glycoprotein. Although the true clinical relevance of multidrug resistance is still heavily debated, MDR1/P-glycoprotein is believed to be one of the key molecules which cause multidrug resistance in cancer.

Mice lacking mdr1/P-glycoprotein showed hypersensitivity to xenobiotic toxins [13]. The plasma levels of orally administered neurotoxic pesticide ivermectin was several-fold higher, whereas the levels in brain were increased almost 100-fold. The increased uptake of orally administered compounds such as vinblastine, digoxin, and paclitaxel were also increased [14]. These studies clearly showed that MDR1/P-glycoprotein is physiologically important in limiting the uptake of xenobiotics and drugs from the gastrointestinal tract, stimulating their excretion from the liver, kidney, and intestine, and moreover protecting the brain by functioning as a blood-brain barrier.

*Address correspondence to this author at the Laboratory of Cellular Biochemistry, Division of Applied Life Sciences, Graduate School of Agriculture, Kyoto University, Kyoto 606-8502;
E-mail: uedak@kais.kyoto-u.ac.jp

1389-2002/04 $45.00+.00

To understand the mechanism of drug efflux by P-glycoprotein and to confer multidrug resistance to cancer cells by preventing the function of P-glycoprotein, much effort has been made and many reviews have been published [15-19]. In this review article, we describe the general structure and functions of MDR1/P-glycoprotein and expression systems using non-mammalian or specialized cells to study its functions.

I. MDR1/P-GLYCOPROTEIN: AN EXPORTER-TYPE ABC PROTEIN

ABC proteins can be divided into several subfamilies based on the type and direction of substrate transport. In microorganisms, the most extensively studied ABC proteins are importers of amino acids, sugars, peptides and ions. These systems typically include a substrate binding periplasmic receptor subunit that delivers the substrate to the membrane-spanning subunits, and two nucleotide-binding subunits as separate polypeptides. The histidine permease complex of *Salmonella typhimurium* [20], and the maltose transporter complex of *Escherichia coli* (*E. coli*) [21] belong to this importer subfamily. In microorganisms, there are also exporter-type ABC proteins. They are involved in the export of hydrophobic drugs, toxins including colicin and hemolysin, capsulepolysaccharide, proteases, lipases, ions and heavy metals from microorganisms [15,22].

In eukaryotes, ABC proteins can be classified into three major groups; transporters, regulators, or channels, based on function. Cystic fibrosis transmembrane conductance regulator (CFTR) is the only ABC protein clearly proven to function as a channel [23-25]. CFTR is a voltage-independent Cl^- channel found in the epithelial cells of many tissues, and plays major roles in regulating Cl^- fluxes. Mutations in CFTR cause cystic fibrosis, one of the most common serious diseases, which affects 1 in 2000-2500 people in northern Europe and the United States. In addition to its Cl^- channel activity, CFTR is also suggested to act as a regulator of both an outwardly-rectifying Cl^- channel (ORCC) and an epithelial Na^+ channel. Numerous abnormalities of cystic fibrosis are believed to be related to this multifunctionality of CFTR [26]. The sulfonylurea receptor (SUR1) was identified as a target protein for sulfonylureas, such as glybenclamide, which is most commonly used in the treatment of non-insulin-dependent diabetes mellitus [27]. SUR1 is a subunit of the pancreatic β-cell K_{ATP} channel. The β-cell K_{ATP} channel is a hetero-octamer composed of pore-forming Kir6.2 subunits and SUR1 that co-assemble with a 4:4 stoichiometry, and plays a key role in the regulation of glucose-induced insulin secretion. SUR1 is suggested not to be a channel or transporter itself, but to be a switch, which regulates the opening and closing of Kir6.2 channel subunits by monitoring the intracellular metabolic state, especially the ADP concentration [17].

Most of the other eukaryotic ABC proteins seem to be transporters, though there are still many members with unknown functions. All the eukaryotic transporter-type ABC proteins, so far studied, transport substrates outwardly from cells. One exception may be a plant MDR-type ABC protein CjMDR1, which is involved in alkaloid transport in *Coptis Japonica* [28]. It is proposed that CjMDR1 is involved in the translocation of berberine from the root to the rhizome, and functions as an influx pump for berberine. MDR1/P-glycoprotein, described in this review, is a prominent member of eukaryotic export-type ABC proteins. MDR1/P-glycoprotein extrudes a very wide array of structurally dissimilar compounds, all lipophilic and ranging in mass from approximately 300 to 2000 Da, including cytotoxic drugs that act on different intracellular targets, steroid hormones, peptide antibiotics, immunosuppressive agents, calcium channel blockers, and others.

II. STRUCTURE OF MDR1/P-GLYCOPROTEIN

II-1. Domain Structure

MDR1/P-glycoprotein consists of four distinct domains (Fig. **1**). Two of these are highly hydrophobic, integral transmembrane domains (TMDs), each of which spans the membrane six times by α-helices. The other two are hydrophilic nucleotide-binding folds (NBFs), which share homology with potential nucleotide binding sites of peripheral membrane components of bacterial active transporter systems. The individual domains are frequently expressed as separate polypeptides in prokaryotic ABC proteins [29], while many eukaryotic ABC proteins have all four domains fused into a single polypeptide as illustrated in (Fig. **1**).

II-2. Conserved Sequence Motifs

All the ABC proteins contain within each NBF at least three highly conserved sequence motifs, the Walker A, Walker B, and the ABC signature sequence, also known as the C motif or a linker sequence. Walker A and B motifs are widely conserved among many nucleotide-binding proteins, such as ras P21 (Ras), RecA, adenylate kinase, myosin and F_1-ATPase. The Walker A motif (Gly-X-X-Gly-X-Gly-Lys-Ser/Thr-Ser/Thr) is also known as a phosphate-binding loop (P-loop) or a glycine-rich loop. Residues within this motif interact with the phosphate groups and the magnesium ion of the bound Mg^{2+}-nucleotide complex. The Walker B motif is h-h-h-h-Asp, where h is a hydrophobic residue. In the structures of ATP- or GTP-binding proteins, this sequence constitutes a buried β-strand within the core of the NBF [30]. The highly conserved aspartate residue is involved in the coordination of the catalytic Mg^{2+} ion. An amino acid substitution of the conserved lysine residue in the Walker A motif or the conserved aspartate residue in the Walker B motif either in NBF results in a loss of the ATP hydrolysis activity of MDR1/P-glycoprotein [31-33]. The glutamate residue next to the aspartate residue of the Walker B motif is also conserved among the ABC proteins. An amino acid substitution of this glutamate residue in the h-h-h-h-Asp-Glu sequence in either of the NBFs also abrogates steady-state ATP hydrolysis and drug transport activities, but does not impair vanadate-dependent nucleotide trapping [34], suggesting that the conserved glutamate residue in the Walker B motif may not be directly involved in ATP hydrolysis but is essential for the second ATP hydrolysis step and completion of the catalytic cycle. Vanadate-induced nucleotide trapping is a unique feature of the ATP hydrolysis cycle of ABC proteins (see section III-3).

The C motif (Leu-Ser-Gly-Gly-Gln-Gln/Arg/Lys-Gln-Arg) exists within each NBF of all the ABC proteins, but not of other nucleotide-binding protein families, such as GTP-

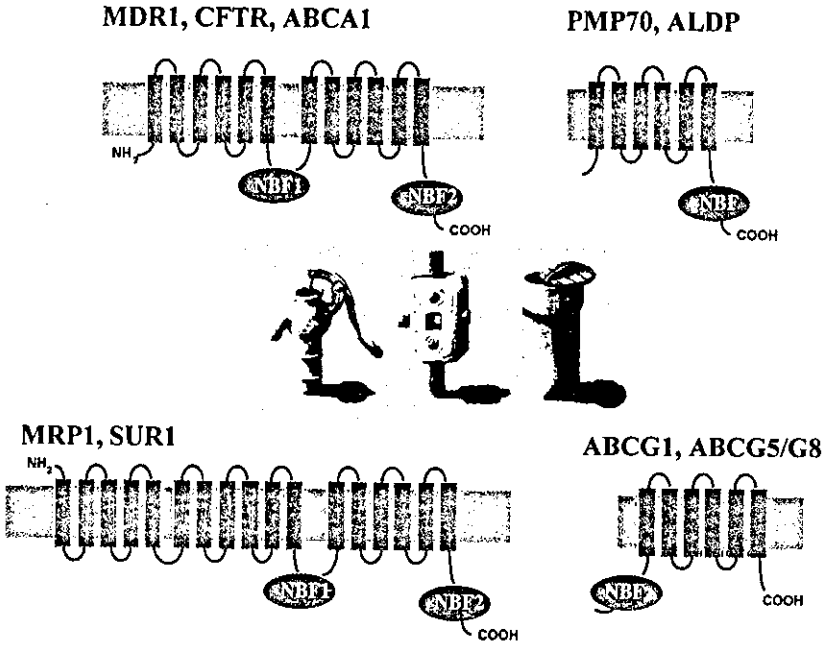

Fig. (1). The predicted secondary structures and functions of eukaryotic ABC proteins.

binding proteins and the AAA superfamily. Therefore, it is also called the ABC signature motif. This motif is located immediately N-terminal to the Walker B motif. The C motif was suggested to be involved in interaction with the membrane domains from the study of the crystal structure of the HisP monomer [35], and it has been suggested that this region is involved in the transduction of the energy of ATP hydrolysis to the conformational changes in the membrane-integral domains required for translocation of the substrate [29]. The crystal structure of the *E. coli* BtuCD protein, an ABC transporter mediating vitamin B12 uptake, was recently determined [36] as described in the next section. The two ATP-binding subunits (BtuD) are in close contact with each other in the crystal structure as predicted by Jones, P. M., and George, A. M. [37], and the ATP molecules are proposed to be sandwiched between the Walker A sequence and the ABC signature motif of opposing BtuD subunits.

Other than the three conserved motifs mentioned above, glutamine located between the Walker A motif and the signature motif is highly conserved among the ABC proteins and the loop containing this glutamine is called the Q-loop [38]. Crystal structure analysis of HisP has suggested that the correspondent glutamine, Gln100, in the HisP molecule is likely to form hydrogen bonds with a water molecule, which interacts with the γ-phosphate of ATP. This water molecule is a candidate for attacking water molecules during ATP hydrolysis [35]. The comparable amino acid substitution, Gln1291Arg, in CFTR was observed in patients with cystic fibrosis, and the Gln1291Arg CFTR shows no chloride channel function although it reaches the plasma membrane as a fully glycosylated mature protein [39]. A missense mutation of the corresponding glutamine in the second NBF of the multidrug resistance protein 2 (MRP2, ABCC2) was detected in a patient with Dubin-Johnson syndrome (DJS), a hereditary disease characterized by hyperbilirubinemia. This mutation caused a lack of substrate-induced vanadate trapping, which may suggest that the glutamine is involved in ATP hydrolysis directly or in the conformational change after ATP hydrolysis. However, because the correspondent glutamine residue in the MalK molecule, the nucleotide binding subunit of the *E. coli* maltose transporter complex, was suggested to be placed too far away from the nucleotide to coordinate Mg^{2+} and the water molecule that attacks the γ-phosphate bond [40], the role of the glutamine in the Q-loop is not yet clear.

II-3. Three Dimensional Structure

An approximately 10 angstrom resolution structure of MDR1/P-glycoprotein was determined by electron cryo-microscopy of two-dimensional crystals [41]. More recently, the three-dimensional structure in the presence and absence of nucleotide was reported at a resolution of approximately 20 angstrom [42]. The TMDs form a chamber within the membrane that appears to be open to the extracellular milieu, and may also be accessible from the lipid phase at the interfaces between the two TMDs. This structure may be consistent with a predicted model for the function of P-glycoprotein and a general architecture for ABC proteins. P-glycoprotein is predicted to act as a 'vacuum cleaner' or a 'flippase' with drug substrates gaining access to their binding site(s) from the inner leaflet of the lipid bilayer [43]. A gap present in the protein ring could allow substrates to access the central pore from the lipid phase. Many mutations, which alter substrate specificity, are scattered throughout the membrane-spanning α-helices, suggesting that several transmembrane α-helices contribute to substrate binding sites [44]. The substrates transported by different ABC proteins can vary widely, from small ions to large polypeptides and polysaccharides. A large pore could readily be adapted to accommodate different sized substrates. The projection structures of P-glycoprotein trapped at different steps of the transport cycle were also determined by Rosenberg *et al.* [41]. ATP binding, not hydrolysis, was proposed to drive the major conformational change

associated with solute translocation. However, crystal structures at a higher resolution are a prerequisite to understand the mechanism of substrate recognition and transport.

Recently, the crystal structure of the *E. coli* BtuCD protein, an ABC transporter mediating vitamin B12 uptake, was reported at a resolution of 3.2 angstrom [36]. The two ATP-binding subunits (BtuD) are in close contact with each other, as are the two membrane-spanning subunits (BtuC). The BtuC subunits provide 20 transmembrane helices grouped around a translocation pathway that is closed to the cytoplasm by a gate region. The ATP molecules are sandwiched between the Walker A motif and the ABC signature (LeuSerGlyGlyGln) motif of opposing BtuD subunits. Because Loo *et al.* reported that the ABC signature motif in each NBF of human MDR1/P-glycoprotein is adjacent to the opposing Walker A sequence based on cross-linking experiments [45], some similar features of structure may be expected for MDR1/P-glycoprotein.

III. NUCLEOTIDE INTERACTION AND HYDROLYSIS BY MDR1/P-GLYCOPROTEIN

Nucleotide binding and hydrolysis by MDR1/P-glycorptrotein is tightly coupled with its function, substrate transport. This is evident by the fact that a mutation that abolishes ATP binding and/or hydrolysis impairs substrate transport by MDR1/P-glycoprotein and photoaffinity labeling of MDR1/P-glycoprotein by iodoarylazidoprazosine (IAAP), which arrests the transport cycle, inhibits ATP hydrolysis. In this section, we focus on the issues of nucleotide interaction and hydrolysis by MDR1/P-glycoprotein.

III-1. Nucleotide Binding by MDR1/P-Glycoprotein

ATP analogs are useful tools for studying the nucleotide-binding properties of MDR1/P-glycoprotein. Liu *et al.* reported that nucleotide analog 2'(3')-O-(2,4,6-trinitrophenyl)-ATP (TNP-ATP) and TNP-ADP bound to MDR1/P-glycoprotein and inhibited ATP hydrolysis [46], indicating that they interact with NBFs of MDR1/P-glycoprotein. The Kd (dissociation constant) values, estimated from increased fluorescence intensity, were 43 and 36 μM for TNP-ATP and TNP-ADP, respectively. Other nucleotide analogs, which are useful for examining the nucleotide binding by MDR1/P-glycoprotein, are photoreactive 8-azido-ATP and 8-azido-ADP [47,48]. MDR1/P-glycoprotein can be photoaffinity labeled with these nucleotide analogs to elucidate functional details. The 8-azido-ATP binding of NBFs of MDR1/P-glycoprotein required a Mg^{2+} ion. Hrycyna *et al.* suggested that the ATP binding of two NBFs is asymmetric, because the labeling was observed predominantly in NBF1 of MDR1/P-glycoprotein [31]. The other way to analyze nucleotide binding is to utilize thiol-reactive fluor, 2-(4-maleimidoanilino)-naphthalene-6-sulfonic acid (MIANS), which covalently modifies a cysteine residue within the Walker A motif [49]. Quenching of the fluorescence was observed on addition of ATP, suggesting that a conformational change takes place due to the ATP binding at NBFs. The quenching occurs in a concentration-dependent manner with a Ki of 370 μM, which is a similar value to the Km for ATP hydrolysis.

III-2. ATP Hydrolysis by MDR1/P-Glycoprotein

There are many reports about the hydrolysis of ATP by MDR1/P-glycoprotein, but the specific ATPase activity of MDR1/P-glycoprotein varies from 1 to 3900 nmol/min/mg protein [50-64]. These differences may depend on the purity, the source (endogenous or exogenously expressed MDR1/P-glycoprotein), the efficiency of reconstitution of MDR1/P-glycoprotein into liposomes, and on the lipid composition of liposomes. If we assume the activity to be 1000 nmol/min/mg protein, the turnover number is $2.4s^{-1}$, which is lower than for other membrane ATPases such as FoF_1-ATPase ($500s^{-1}$) [65] but higher than for chaperonin HSP70 (from $3x10^{-3}$ to $1.6x10^{-2}s^{-1}$) [66]. In any case, verapamil stimulated ATPase activity 2- to 10-fold with an EC_{50} of 2-3 μM and vinblastine stimulated it 2- to 5-fold with an EC_{50} of 1 μM [57,59,63]. Other substrates including colchicines, daunomycin, trifluoperazine, amiodarone, nifedipine and actinomycinD, also stimulated the hydrolysis of ATP by MDR1/P-glycoprotein [50,51,56,62-64]. It is not clear that all substances transported by MDR1/P-glycoprotein stimulate ATP hydrolysis, but most seem to. One can assume that drug-stimulated ATP hydrolysis is applicable to screening for drugs that are transported by MDR1/P-glycoprotein. In fact, such a screening system is commercially available from GENTEST Co. Ltd. In this system, MDR1/P-glycoprotein expressed in insect cells, is used to evaluate the ability of a drug to stimulate ATPase activity. Several substances have been reported to inhibit hydrolysis of ATP by MDR1/P-glycoprotein. Modification of the cysteine residue within the Walker A motif by NEM inhibits the ATPase activity with Ki= 5-6 μM, possibly via steric hindrance of entry of ATP into a nucleotide-binding pocket [32,51,63]. Orthovanadate, an inhibitor of ATP hydrolysis mediated by myosin and P-type ATPase, exhibits Ki=2-3 μM for MDR1/P-glycolprotein [57-59]. One may expect a specific inhibitor of hydrolysis of ATP by MDR1/P-glycoprotein to overcome the multidrug resistance of cancer cells, but no such drug has been found.

III-3. Vanadate-Induced Nucleotide Trapping of MDR1/P-Glycoprotein

Vanadate-induced nucleotide trapping has been studied extensively using myosin [67,68] and was first applied to study MDR1/P-glycoprotein by Urbatsch *et al.* [69,70]. We developed a simple procedure for detecting vanadate-induced nucleotide trapping and applied it to the study of MDR1/P-glycoprotein and other ABC proteins [32,71-73]. Orthovanadate (Vi) is an analog of inorganic phosphate and a stable inhibitory complex is generated by trapping MgADP-Vi at the catalytic site after the hydrolysis of ATP by MDR1/P-glycoprotein (Fig. 2). When MDR1 is incubated with 8-azido-[^{32}P]ATP and orthovanadate, it forms a metastable complex (MDR1-Mg 8-azido-ADP-Vi) after hydrolysis. Upon UV-irradiation, MDR1/P-glycoprotein is photoaffinity-labeled with 8-azido-[^{32}P]ATP.

Beryllium fluoride (BeFx), an inhibitor of F_1-ATPase and myosin, is another analog of inorganic phosphate which acts like orthovanadate, though in the metastable state it mimics the Mg-ATP-bound form rather than the transition state for hydrolysis [74]. Sankaran *et al.* reported that beryllium

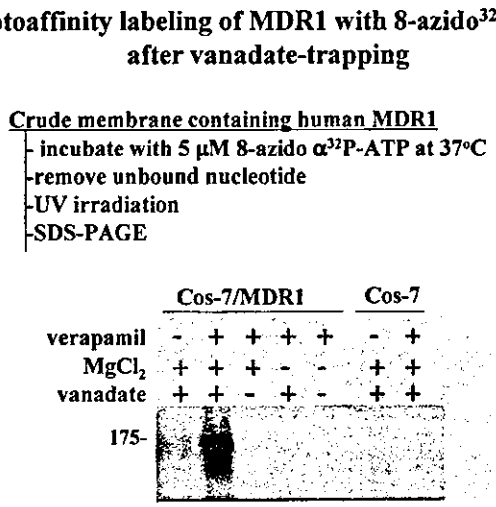

Fig. (2). Photoaffinity labeling of MDR1 with 8-azido^{32}P-ATP after vanadate-trapping.

fluoride-induced nucleotide trapping also occurs in MDR1/P-glycoprotein [75]. With these methods, it is possible to detect the hydrolysis of a single ATP during the catalytic cycle, and the density of labeling reflects the ATPase activity of MDR1/P-glycoprotein.

Urbatsch *et al.* showed that the two NBFs of MDR1/P-glycoprotein hydrolyze ATP, because both the N- and C-terminal halves, produced by mild trypsin digestion, were photoaffinity-labeled [70]. Mutation of the Walker A lysine or NEM modification of the Walker A cysteine in either of the NBFs abolished the vanadate-induced nucleotide trapping of both NBFs, suggesting that the two NBFs function cooperatively [32]. The advantage of this method is that the purified MDR1/P-glycoprotein is not required and that the specific ATP hydrolysis by MDR1/P-glycprotein can be detected by using crude membranes from cells, in which MDR1/P-glycoprotein is functionally expressed. Photoaffinity-labeled MDR1/P-glycoprotein is separated by the SDS-PAGE of crude membranes and detected by autoradiography. There are no proteins, larger than 80 kDa, which show vanadate-induced nucleotide trapping in HEK293, Cos-7, and KB-3-1 cells. The labeling is induced by the presence of drugs such as verapamil and vinblastine. Therefore, vanadate-induced nucleotide trapping is a useful method of detecting drug-induced ATP hydrolysis by MDR1/P-glycoprotein, and may be suitable for high throughput screening of drugs. One of the main drawbacks of this method would be the costliness of ^{32}P-labeled 8-azide-modified nucleotides.

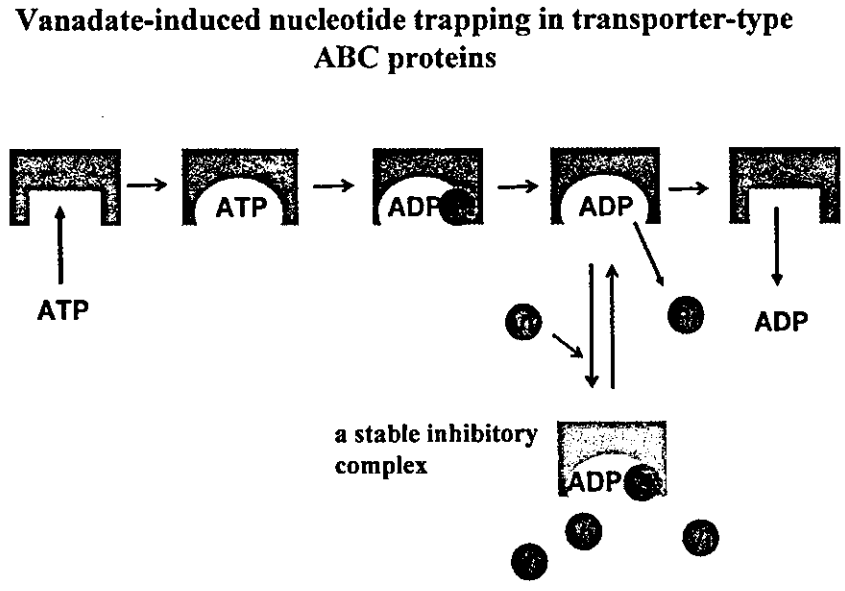

Fig. (3). Schematic diagram of Vanadate-induced nucleotide trapping in transporter-type ABC proteins.

III-4. Coupling of ATP Hydrolysis and Drug Transport

The molecular mechanism of energy coupling to substrate transport of MDR1/P-glycoprotein is not clear. It is evident, however, that ATP hydrolysis provides the driving force for substrate transport, because a mutation or chemical modification that abolishes the hydrolysis impairs substrate transport and because non-hydrolysable ATP analogs such as ATP-γS do not support substrate transport.

Two NBFs seem to function cooperatively and hydrolyze ATP in order, although it is not clear which NBF hydrolyzes ATP first. At first, drug binds to the high-affinity drug-binding site of the cytosolic side (or inner membrane leaflet) of MDR1/P-glycoprotein. ATP hydrolysis causes conformational change, which releases the drug from the low-affinity drug-binding site facing the extracellular side. Sauna *et al.* showed that ATP binding *per se* did not affect interactions with substrate (IAAP) but that the affinity of IAAP was reduced in the vanadate-induced nucleotide trapped state (MDR1-MgADP-Vi) [76]. To transform MDR1/P-glycoprotein to recover the high affinity IAAP, binding required conditions that permit ATP hydrolysis. They proposed that the first ATP hydrolysis functions in the transport of substrate and the second in conformational change to reset MDR1/P-glycoprotein for the next catalytic cycle. In this model, two ATP molecules are hydrolyzed for the transport of one substrate molecule. However, the stoichiometry of ATP hydrolysis and substrate transport is in dispute. Partly, it is difficult to reconstitute the purified functional P-glycoprotein in liposomes with 100% efficiency and to measure transported hydrophobic substrates for P-glycoprotein accurately.

IV. HETEROLOGOUS EXPRESSION SYSTEMS TO STUDY MDR1/P-GLYCOPROTEINS

The biochemical data helped us to understand the mechanism of action of MDR1/P-glycoprotein, but visualization of the structure is needed to fully understand how MDR1/P-glycoprotein recognizes such a variety of compounds and how it carries its substrates across the membrane using the energy from ATP hydrolysis. To visualize the structure, namely to obtain a 3D crystal for structural determination, large amounts of pure and stable proteins are required. In this section, heterologous expression systems, which have been used to express P-glycoprotein, are described.

IV-1. Expression in *E. Coli*

The simple and rapid life cycle of *E. coli* makes it attractive for the acquisition of purified proteins in quantities sufficient for biochemical and structural studies, for the large-scale screening of substrates and modulators, and for mutagenesis studies. However, only limited success in the functional expression of MDR1/P-glycoprotein in *E. coli* has been reported. A major problem is several proteases in *E. coli*, which recognize and degrade foreign proteins such as P-glycoprotein. Another is the toxic effect of eukaryotic ABC proteins on *E. coli*. A protease-deficient mutant strain and a relatively weak lac/promoter-operator system were successfully used for the functional expression of the mouse mdr1 [77]. Nevertheless, the expression of mouse mdr3 and human MDR1 was unsuccessful using the same expression system [78]. Functional expression of the human MDR1/P-glycoprotein in *E. coli* was reported using the lambda promoter/repressor system [79].

We have tried to express the human MDR1/P-glycoprotein as a fusion protein with *E. coli* β-galactosidase. This fusion protein, fully functional as a drug efflux pump when expressed in NIH3T3 cells [52], was expressed in *E. coli* BL21 (unpublished results). Pale blue colonies of *E. coli* expressing a low level of the human MDR1/P-glycoprotein-β-galactosidase fusion protein showed low levels of resistance to adriamycin and daunomycin. However, induction of the fusion protein with IPTG of concentrations higher than 50 μM inhibited the growth of *E.coli* probably because a high level of expression of the fusion protein was toxic to *E. coli*.

As described above, the main problem of expression in *E. coli* stems from the toxic effect of eukaryotic ABC proteins even when expressed at a low level. This problem must be solved if *E. coli* is to be used as a host for the production of eukaryotic ABC proteins and for drug screening purposes.

IV-2. Expression in Yeasts

Saccharomyces cerevisiae have been successfully used as a host for the functional analysis of P-glycoprotein. Three mouse mdr/P-glycoproteins were expressed in the membranes of secretory vesicles accumulating in a yeast secretion mutant strain [80]. The expression of mdr1 and mdr3, but not mdr2, caused an increased vinblastine accumulation in the vesicles. MDR2/P-glycoprotein is highly expressed in the bile canalicular membrane of hepatocytes, and has an essential role in the secretion of phosphatidylcholine into bile. The function of human MDR2 was also examined using yeast. Interestingly, both human MDR1 and MDR2 conferred resistance to aureobasidin A, a cyclic depsipeptide antifungal antibiotic, in drug-sensitive yeast strains [81]. The resistance to aureobasidin A conferred by both MDR was overcome by vinblastine, verapamil, and cyclosporin A, but not by colchicine, suggesting that human MDR1 and MDR2 have conserved domain(s) for drug recognition. Because human MDR2 (often called MDR3/P-glycoprotein) shares about 80% identity at the amino acid level with MDR1/P-glycoprotein, it is conceivable that they share conserved domain(s) for drug recognition. However, mouse mdr1 and mdr3 were not able to compensate for the physiological function of mdr2 in the mdr2(-/-) mice, although mdr1 and mdr3 were expressed at elevated levels [82]. Therefore, although MDR1 and MDR2 have conserved domain(s) for drug recognition, it is suggested that MDR1/P-glycoprotein is not good at secreting phosphatidylcholine into the bile, and MDR2/P-glycoprtein is not good at transporting anticancer drugs.

Because the expression levels of mouse and human MDR in *S. cerevisiae* were not high enough to obtain a large amount of pure protein, *Pichia pastoris* (*P. pastoris*) was used for high-level expression of mouse mdr3/P-glycoprotein [83]. *P. pastoris* is a methylotrophic yeast capable of metabolizing methanol as a sole carbon source. The first enzyme in the methanol utilization pathway is alcohol oxygenase (AOX1), which converts methanol to formaldehyde. When *P. pastoris* cells are grown with methanol as a

sole carbon source, the AOX1 protein is produced and accounts for 30% of total protein. Therefore, the strong inducible promoter of the AOX1 gene is suitable for an expression system to overproduce foreign proteins. Stable and high-level expression of mouse mdr3/P-glycoproein has been achieved in the membrane fraction of *P. pastoris* [83]. The efficient isolation of a high-purity mouse mdr3/P-glycoprotein and drug-stimulated ATPase activity of the purified mdr3/P-glycoprotein have been reported [84].

IV-3. Expression in Insect Cells

Baculoviruses have become a popular system for over-producing recombinant proteins. The baculovirus-based system is a eukaryotic expression system and thus is expected to use many of the protein modification, processing, and transport systems common to higher eukaryotic cells. Indeed, the majority of the overproduced protein remains soluble in insect cells in contrast to the insoluble proteins obtained from bacteria. *Trichoplusia ni* (High Five)(HF) cells and *Spodoptera frugiperda* (Sf9) cells have been successfully used to express human MDR1/P-glycoprotein [59,85-87]. Rao [85], Szabo *et al.* [87], and Muller *et al.* [86] have expressed human MDR1/P-glycoprotein in insect cells, and succeeded in measuring its activity. However, crude membrane was used to measure the ATPase activity and no purification was attempted in these studies. Only one report [59] has described the ATPase activity of MDR1/P-glycoprotein purified from the insect cells.

Recently, we succeeded in overproducing human MDR1/P-glycoprotein in Sf9 cells, and we purified it (Kimura *et al.* in preparation). The purified MDR1/P-glycoprotein was reconstituted in liposomes and ATPase activity was examined. In contrast to the previous reports on the ATPase activity of human and hamster P-glycoprotein, we could not detect a basal level ATPase activity in our reconstituted human MDR1/P-glycoprotein. The ATPase activity was dependent on the presence of substrate. (Fig. 4) shows the ATPase activity in the presence of verapamil, which is known as an inhibitor of P-glycoprotein but is also a good

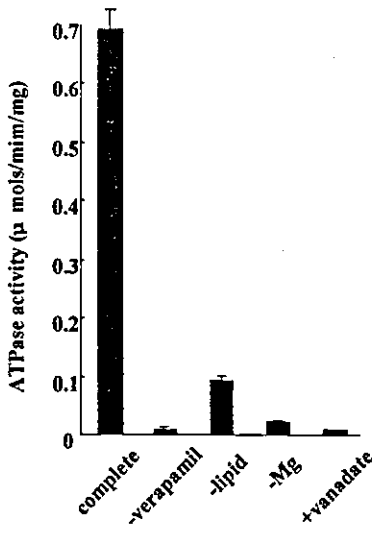

Fig. (4). The ATPase activity of the purified human MDR1/P-glycoprotein.

transport substrate for MDR1/P-glycoprotein as described in section V-3. Verapamil-stimulated ATPase activity of the purified P-glycoprotein is completely inhibited by ortho-vanadate. Although the baculovirus-based system is very efficient in overproducing eukaryotic proteins, we found that insect cells sometimes become incompetent in producing exogenous proteins for unknown reasons, and that the overproduced proteins become insoluble with detergent (Kimura *et al.* unpublished observations). These problems must be solved if baculovirus-based systems are to become more convenient and popular for overproducing eukaryotic integral membrane proteins.

V. TRANSEPITHELIAL TRANSPORT SYSTEM

Stimulation of the ATPase activity of the purified MDR1/P-glycoprotein may be a good test for transported substrates. However, the degree of stimulation and profile of concentration dependence of ATPase activity differ for each chemical and, furthermore, it is not yet clear whether all the transported substrates stimulate the ATPase activity of human MDR1/P-glycoprotein, or whether chemicals that do not stimulate the ATPase activity of human MDR1/P-glycoprotein are not transported inevitably. One convincing way to judge if some chemicals are transported by MDR1/P-glycoprotein would be to use the transepithelial transport system described below.

V-1. Establishment of Transepithelial Transport System

Because the majority of transport substrates for P-glycoprotein are very lipophilic, it is often difficult to determine whether candidate substrates are really transported by P-glycoprotein or not. To solve this problem, we established a transepithelial transport system (Fig. 5A) [88,89]. *MDR1* cDNA isolated from human normal adrenal gland [10] was introduced into LLC-PK1 cells, which are derived from porcine kidney proximal tubules. LLC-PK1 cells form a highly polarized epithelium, and the polarized transport of nutrients and xenobiotic compounds across cultured epithelia has been well documented. P-glycoprotein expressed in the plasma membrane of LLC-GA5-COL300, which was selected in 300 ng/ml colchicine, was detected as a 170-kDa mature form by Western blot analysis using anti-P-glycoprotein monoclonal antibody C219, and was photoaffinity-labeled by [^{3}H]azidopine, a transport substrate for MDR1/P-glycoprotein. LLC-PK1 host cells express a marginal level of porcine P-glycoprotein. Immunostaining using a monoclonal antibody MRK16 that reacts selectively with human P-glycoprotein confirmed the high expression of human P-glycoprotein in the plasma membrane of LLC-GA5-COL300, and electron microscopic immunocyto-chemistry using MRK16 showed that human P-glycoprotein is specifically expressed on the apical surface of the cells as previously reported using MDCK as a host cell [90].

V-2. Transepithelial Transport of Anticancer Drugs

The substrates for P-glycoprotein are highly lipophilic, and so enter cells freely through both surfaces. If there is no specific transport system, basal to apical and apical to basal transport will be the same. However, because human P-glycoprotein localizes specifically in the apical plasma

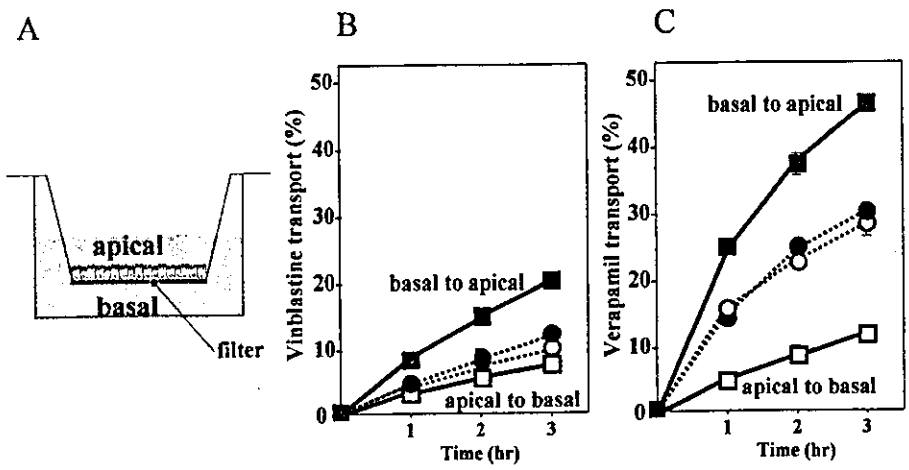

Fig. (5). Scheme illustrating the transcellular transport system (A) and the transcellular transport of vinblastine (B) and verapamil (C) in LLC-PK_1 (circles) and LLC-GA5-COL300 (squares) monolayers.

membrane in LLC-GA5-COL300 cells, substrates for P-glycoprotein entering the cell from the basal surface will be expelled from the apical surface, and those entering the apical plasma membrane are likely to be caught and pumped back into the medium by P-glycoprotein, resulting in a net basal to apical flow of substrates. In LLC-GA5-COL300 cells, basal to apical transport of vinblastine increased about 2-fold and apical to basal transport decreased 1.5- to 2-fold compared to transport in LLC-PK1 cells, resulting in a 6- to 10-fold higher net basal to apical transport (Fig. **5B**).

V-3. Transepithelial Transport of Various Chemicals

By using this transepithelial transport system, the transport of various chemicals by human MDR1/P-glycoprotein was measured. Steroid hormones, such as cortisol, aldosterone, and dexamethasone, were transported, but progesterone was not transported by human MDR1/P-glycoprotein [88]. Digoxin, the most commonly used cardiac glycoside for the treatment of congestive heart failure, was determined to be a good transport substrate for MDR1/P-glycoprotein [89]. Among MDR-reversing agents, cyclosporin A, FK506, azidopine, diltiazem [91,92] and verapamil (Fig. **5C**) were determined to be transported by human MDR1/P-glycoprotein.

Cyclosporin A, a cyclic undecapeptide with highly immunosuppressive effects, efficiently overcomes the multidrug resistance of cancer cells [93,94], and efficiently blocks the transcellular transport of anticancer drugs, steroids, and digoxin. However, verapamil or vinblastine had no obvious effect on the transcellular transport of cyclosporin A [91]. Cyclosporin A may interact with a key site of P-glycoprotein for transport with high affinity. This may be one of the reasons that cyclosporin A is an efficient modulator of P-glycoprotein.

ABBREVIATIONS

ABC	=	ATP-binding cassette
ADP	=	Adenosine-5'-diphosphate
ATP	=	Adenosine-5'-triphosphate
AOX	=	Alcohol oxygenase
CFTR	=	Cystic fibrosis transmembrane conductance regulator
IAAP	=	Iodoarylazidoprazosine
IPTG	=	Isopropyl-β-D-thiogalactoside
K_{ATP} channel	=	ATP-sensitive K^+ channel
Kir	=	Inwardly rectifying K^+ channel
MDR	=	Multidrug resistance
NBF	=	Nucleotide-binding fold
NEM	=	N-ethylmaleimide
SUR	=	Sulfonylurea receptor
TM	=	Transmembrane
TMD	=	Transmembrane domain
3D	=	3-dimensional

REFERENCES

[1] Juliano, R.L. and Ling, V. (1976) *Biochim. Biophys. Acta*, **455**, 152-162.
[2] Roninson, I.B.; Abelson, H.T.; Housman, D.E.; Howell, N. and Varshavsky, A. (1984) *Nature*, **309**, 626-8.
[3] Fojo, A.T.; Whang-Peng, J.; Gottesman, M.M. and Pastan, I. (1985) *Proc. Natl. Acad. Sci. USA*, **82**, 7661-5.
[4] Chen, C.; Chin, J.E.; Ueda, K.; Clark, D.P.; Pastan, I.; Gottesman, M.M. and Roninson, I.B. (1986) *Cell*, **47**, 381-389.
[5] Ueda, K.; Cardarelli, C.; Gottesman, M.M. and Pastan, I. (1987) *Proc. Natl. Acad. Sci. USA*, **84**, 3004-3008.
[6] Ueda, K.; Cornwell, M.M.; Gottesman, M.M.; Pastan, I.; Roninson, I.B.; Ling, V. and Riordan, J.R. (1986) *Biochem. Biophys. Res. Commun.*, **141**, 956-962.
[7] Gros, P.; Croop, J. and Housman, D. (1986) *Cell*, **47**, 371-380.
[8] Riordan, J.R.; Deuchars, K.; Kartner, N.; Alon, N.; Trent, J. and Ling, V. (1985) *Nature*, **316**, 817-9.
[9] Choi, K.; Chen, C.; Kriegler, M. and Roninson, I.B. (1988) *Cell*, **53**, 519-529.
[10] Kioka, N.; Tsubota, J.; Kakehi, Y.; Komano, T.; Gottesman, M.M.; Pastan, I. and Ueda, K. (1989) *Biochem. Biophys. Res. Commun.*, **162**, 224-231.
[11] Gros, P.; Niriah, Y.B.; Croop, J.M. and Housman, D.E. (1986) *Nature*, **323**, 728-731.

[12] Pastan, I.; Gottesman, M.M.; Ueda, K.; Lovelace, E.; Rutherford, A.V. and Willingham, M.C. (1988) *Proc. Natl. Acad. Sci. USA*, **85**, 4486-4490.
[13] Schinkel, A.H.; Smit, J.J.; Tellingen, O.v.; Beijnen, J.H.; Wagenaar, E.; Deemter, L.v.; Mol, C.A.; Valk, M.A.v.D.; Robanus-Maandag, E.C.; Riele, H.P.T.; Berns, A.J.M. and Borst, P. (1994) *Cell*, **77**, 491-502.
[14] Schinkel, A.H. (1997) *Semin. Cancer Biol.*, **8**, 161-70.
[15] Higgins, C.F. (1992) *Annu. Rev. Cell Biol.*, **8**, 67-113.
[16] Gottesman, M.M. and Pastan, I. (1993) *Annu. Rev. Biochem.*, **62**, 385-427.
[17] Ueda, K.; Matsuo, M.; Tanabe, K.; Kioka, N. and Amachi, T. (1999) *Biochim. Biophys. Acta*, **1461**, 305-313.
[18] Loo, T.W. and Clarke, D.M. (1999) *Biochim. Biophys. Acta*, **1461**, 315-25.
[19] Sharom, F.J.; Liu, R.; Romsicki, Y. and Lu, P. (1999) *Biochim. Biophys. Acta*, **1461**, 327-45.
[20] Doige, C.A. and Ames, G.F. (1993) *Annu. Rev. Microbiol.*, **47**, 291-319.
[21] Ehrmann, M.; Ehrle, R.; Hofmann, E.; Boos, W. and Schlosser, A. (1998) *Mol. Microbiol.*, **29**, 685-94.
[22] Fath, M.J. and Kolter, R. (1993) *Microbiol. Rev.*, **57**, 995-1017.
[23] Welsh, M.J.; Anderson, M.P.; Rich, D.P.; Berger, H.A.; Denning, G.M.; Ostedgaard, L.S.; Sheppard, D.N.; Cheng, S.H.; Gregory, R.J. and Smith, A.E. (1992) *Neuron*, **8**, 821-9.
[24] Riordan, J.R. (1993) *Annu. Rev. Physiol.*, **55**, 609-30.
[25] Gadsby, D.C.; Nagel, G. and Hwang, T.C. (1995) *Annu. Rev. Physiol.*, **57**, 387-416.
[26] Tsui, L.C. and Buchwald, M. (1991) *Adv. Hum. Genet.*, **20**, 153-266, 311-2.
[27] Aguilar-Bryan, L.; Nichols, C.G.; Wechsler, S.W.; Clement, J.P.I.; Boyd, A.E.I.; Gonzalez, G.; Herrera-Sosa, H.; Nguy, K.; Bryan, J. and Nelson, D.A. (1995) *Science*, **268**, 423-426.
[28] Shitan, N.; Bazin, I.; Dan, K.; Obata, K.; Kigawa, K.; Ueda, K.; Sato, F.; Forestier, C. and Yazaki, K. (2003) *Proc. Natl. Acad. Sci. USA*, **100**, 751-756.
[29] Hyde, S.C.; Emsley, P.; Hartshorn, M.J.; Mimmack, M.M.; Gileadi, U.; Pearce, S.R.; Gallagher, M.P.; Gill, D.R.; Hubbard, R.E. and Higgins, C.F. (1990) *Nature*, **346**, 362-365.
[30] Smith, C.A. and Rayment, I. (1996) *Biophys. J.*, **70**, 1590-602.
[31] Hrycyna, C.A.; Ramachandra, M.; Germann, U.A.; Cheng, P.W.; Pastan, I. and Gottesman, M.M. (1999) *Biochemistry*, **38**, 13887-99.
[32] Takada, Y.; Yamada, K.; Taguchi, Y.; Kino, K.; Matsuo, M.; Tucker, S.J.; Komano, T.; Amachi, T. and Ueda, K. (1998) *Biochim. Biophys. Acta*, **1373**, 131-136.
[33] Urbatsch, I.L.; Beaudet, L.; Carrier, I. and Gros, P. (1998) *Biochemistry*, **37**, 4592-4602.
[34] Sauna, Z.E.; Muller, M.; Peng, X.H. and Ambudkar, S.V. (2002) *Biochemistry*, **41**, 13989-4000.
[35] Hung, L.-W.; Wang, I.X.; Nikaido, K.; Liu, P.Q.; Ames, G.; Fand S.H. Kim (1998) *Nature*, **396**, 703-707.
[36] Locher, K.P.; Lee, A.T. and Rees, D.C. (2002) *Science*, **296**, 1091-8.
[37] Jones, P.M. and George, A.M. (1999) *FEMS Microbiol. Lett.*, **179**, 187-202.
[38] Hopfner, K.; Karcher, A.; Shin, D.S.; Craig, L.; Arthur, L.M.; Carney, J.P. and Tainer, J.A. (2000) *Cell*, **101**, 789-800.
[39] Dork, T.; Mekus, F.; Schmidt, K.; Bosshammer, J.; Fislage, R.; Heuer, T.; Dziadek, V.; Neumann, T.; Kalin, N.; Wulbrand, U. and *et al.* (1994) *Hum. Genet.*, **94**, 533-42.
[40] Diederichs, K.; Diez, J.; Greller, G.; Muller, C.; Breed, J.; Schnell, C.; Vonrhein, C.; Boos, W. and Welte, W. (2000) *EMBO J.*, **19**, 5951-5961.
[41] Rosenberg, M.F.; Velarde, G.; Ford, R.C.; Martin, C.; Berridge, G.; Kerr, I.D.; Callaghan, R.; Schmidlin, A.; Wooding, C.; Linton, K.J. and Higgins, C.F. (2001) *EMBO J.*, **20**, 5615-25.
[42] Rosenberg, M.F.; Kamis, A.B.; Callaghan, R.; Higgins, C.F. and Ford, R.C. (2003) *J. Biol. Chem.*, **278**, 8294-8299.
[43] Higgins, C.F. and Gottesman, M.M. (1992) *Trends Biochem. Sci.*, **17**, 18-21.
[44] Ueda, K.; Taguchi, Y. and Morishima, M. (1997) in: Seminars in Cancer Biology, pp. 151-160 (Borst, P.; Ed.) Academic Press, UK.
[45] Loo, T.W.; Bartlett, M.C. and Clarke, D.M. (2002) *J. Biol. Chem.*, **277**, 41303-6.
[46] Liu, R. and Sharom, F.J. (1997) *Biochemistry*, **36**, 2836-2843.
[47] Azzaria, M.; Schurr, E. and Gros, P. (1989) *Mol. Cell. Biol.*, **9**, 5289-5297.
[48] Al-Shawi, M.K.; Urbatsch, I.L. and Senior, A.E. (1994) *J. Biol. Chem.*, **269**, 8986-8992.
[49] Liu, R. and Sharom, F.J. (1996) *Biochemistry*, **35**, 11865-11873.
[50] Ambudkar, S.V.; Lelong, I.H.; Zhang, J.; Cardarelli, C.O.; Gottesman, M.M. and Pastan, I. (1992) *Proc. Natl. Acad. Sci. USA*, **89**, 8472-8476.
[51] Shapiro, A.B. and Ling, V. (1994) *J. Biol. Chem.* **269**, 3745-3754.
[52] Shimabuku, A.M.; Nishimoto, T.; Ueda, K. and Komano, T. (1992) *J. Biol. Chem.*, **267**, 4308-4311.
[53] Hamada, H. and Tsuruo, T. (1988) *J. Biol. Chem.*, **263**, 1454-1458.
[54] Dong, M.; Penin, F. and Baggetto, L.G. (1996) *J. Biol. Chem.*, **271**, 28875-28883.
[55] Doige, C.A.; Yu, X. and Sharom, F.J. (1993) *Biochim. Biophys. Acta*, **23**, 65-72.
[56] Doige, C.A.; Yu, X. and Sharom, F.J. (1992) *Biochim. Biophys. Acta*, **1109**, 149-160.
[57] Rosenberg, M.F.; Callaghan, R.; Ford, R.C. and Higgins, C.F. (1997) *J. Biol. Chem.*, **272**, 10685-10694.
[58] Callaghan, R.; Berridge, G.; Ferry, D.R. and Higgins, C.F. (1997) *Biochimica et Biophysica Acta (BBA) – Biomembranes*, **1328**, 109-124.
[59] Ramachandra, M.; Ambudkar, S.V.; Chen, D.; Hrycyna, C.A.; Dey, S.; Gottesman, M.M. and Pastan, I. (1998) *Biochemistry*, **37**, 5010-9.
[60] Mao, Q.; Leslie, E.M.; Deeley, R.G. and Cole, S.P.C. (1999) *Biochim. Biophys. Acta*, **1461**, 69-82.
[61] Sharom, F.J.; Yu, X. and Doige, C.A. (1993) *J. Biol. Chem.*, **268**, 24197-24202.
[62] Sharom, F.J.; Yu, X.; Chu, J.W. and Doige, C.A. (1995) *Biochem. J.*, **308**, 381-90.
[63] Urbatsch, I.L.; Al-Shawi, M.K. and Senior, A.E. (1994) *Biochemistry*, **33**, 7069-70756.
[64] Loo, T.W. and Clarke, D.M. (1995) *J. Biol. Chem.*, **270**, 21449-21452.
[65] Weber, J. and Senior, A.E. (1997) *Biochim. Biophys. Acta*, **1319**, 19-58.
[66] Ha, J.-H.; Johnson, E.R.; McKay, D.B.; Sousa, M.C.; Takeda, S. and Wilbanksm, S.M. (1999), pp. 573-607 (Bukau, B.; Ed.) Harwood Academic Publishers, Amsterdam.
[67] Goodno, C.C. (1979) *Proc. Natl. Acad. Sci. USA*, **76**, 2620-4.
[68] Goodno, C.C. and Taylor, E.W. (1982) *Proc. Natl. Acad. Sci. USA*, **79**, 21-5.
[69] Urbatsch, I.L.; Sankaran, B.; Weber, J. and Senior, A.E. (1995) *J. Biol. Chem.*, **270**, 19383-19390.
[70] Urbatsch, I.L.; Sankaran, B.; Bhagat, S. and Senior, A.E. (1995) *J. Biol. Chem.*, **270**, 26956-26961.
[71] Taguchi, Y.; Yoshida, A.; Takada, Y.; Komano, T. and Ueda, K. (1997) *FEBS Lett.*, **401**, 11-14.
[72] Hashimoto, K.; Uchiumi, T.; Konno, T.; Ebihara, T.; Nakamura, T.; Wada, M.; Sakisaka, S.; Maniwa, F.; Amachi, T.; Ueda, K. and Kuwano, M. (2002) *Hepatology*, **36**, 1236-1245.
[73] Nagata, K.; Nishitani, M.; Matsuo, M.; Kioka, N.; Amachi, T. and Ueda, K. (2000) *J. Biol. Chem.*, **275**, 17626-17630.
[74] Fisher, A.J.; Smith, C.A.; Thoden, J.B.; Smith, R.; Sutoh, K.; Holden, H.M. and Rayment, I. (1995) *Biochemistry*, **34**, 8960-72.
[75] Sankaran, B.; Bhagat, S. and Senior, A.E. (1997) *Biochemistry*, **36**, 6847-6853.
[76] Sauna, Z.E. and Ambudkar, S.V. (2000) *Proc. Natl. Acad. Sci. USA*, **97**, 2515-20.
[77] Bibi, E.; Gros, P. and Kaback, H.R. (1993) *Proc. Natl. Acad. Sci. USA*, **90**, 9209-13.
[78] Bibi, E.; Edgar, R. and Beja, O. (1998) *Methods Enzymol.*, **292**, 370-82.
[79] George, A.M.; Davey, M.W. and Mir, A.A. (1996) *Arch. Biochem. Biophys.*, **333**, 66-74.
[80] Ruetz, S. and Gros, P. (1994) *J. Biol. Chem.*, **269**, 12277-84.
[81] Kino, K.; Taguchi, Y.; Yamada, K.; Komano, T. and Ueda, K. (1996) *FEBS Lett.*, **399**, 29-32.
[82] Smit, J.J.M.; Schinkel, A.H.; Oude Elferink, R.P.J.; Groen, A.K.; Wagenaar, E.; van Deemter, L.; Mol, C.A., A. M.; Ottenhoff, R.; van der Lugt, N.M.T.; van Roon, M.A.; van der Valk, M.A.; Offerhaus, G.J.A.; Berns, A.J.M. and Borst, P. (1993) *Cell*, **75**, 451-462.

[83] Beaudet, L.; Urbatsch, I.L. and Gros, P. (1998) *Methods Enzymol.*, **292,** 397-413.
[84] Julien, M.; Kajiji, S.; Kaback, R.H. and Gros, P. (2000) *Biochemistry,* **39,** 75-85.
[85] Rao, U.S. (1995) *J. Biol. Chem.*, **270,** 6686-90.
[86] Muller, M.; Bakos, E.; Welker, E.; Varadi, A.; Germann, U.A.; Gottesman, M.M.; Morse, B.S.; Roninson, I.B. and Sarkadi, B. (1996) *J. Biol. Chem.*, **271,** 1877-1883.
[87] Szabo, K.; Welker, E.; Bakos, E.; Muller, M.; Roninson, I.; Varadi, A. and Sarkadi, B. (1998) *J. Biol. Chem.*, **273,** 10132-8.
[88] Ueda, K.; Okamura, N.; Hirai, M.; Tanigawara, Y.; Saeki, T.; Kioka, N.; Komano, T. and Hori, R. (1992) *J. Biol. Chem.*, **267,** 24248-24252.
[89] Tanigawara, Y.; Okamura, N.; Hirai, M.; Yasuhara, M.; Ueda, K.; Kioka, N.; Komano, T. and Hori, R. (1992) *J. Pharmacol. Exp. Ther.*, **263,** 840-845.
[90] Horio, M.; Chin, K.-V.; Currier, S.J.; Goldenberg, S.; Williams, C.; Pastan, I.; Gottesman, M.M. and Handler, J. (1989) *J. Biol. Chem.*, **264,** 14880-14884.
[91] Saeki, T.; Ueda, K.; Tanigawara, Y.; Hori, R. and Komano, T. (1993) *J. Biol. Chem.*, **268,** 6077-6080.
[92] Saeki, T.; Ueda, K.; Tanigawara, Y.; Hori, R. and Komano, T. (1993) *FEBS Lett.*, **324,** 99-102.
[93] Slater, L.M.; Sweet, P.; Stupecky, M. and Gupta, S. (1986) *J. Clin. Invest.*, **77,** 1405-1408.
[94] Twentyman, P.R. (1992) *Biochem. Pharmacol.*, **43,** 109-117.

Available online at www.sciencedirect.com
SCIENCE DIRECT®
Biochemical and Biophysical Research Communications 324 (2004) 262–268
BBRC
www.elsevier.com/locate/ybbrc

Human ABCA3, a product of a responsible gene for *abca3* for fatal surfactant deficiency in newborns, exhibits unique ATP hydrolysis activity and generates intracellular multilamellar vesicles☆

Koh Nagata[a], Akitsugu Yamamoto[b], Nobuhiro Ban[c], Arowu R. Tanaka[a], Michinori Matsuo[a], Noriyuki Kioka[a], Nobuya Inagaki[c], Kazumitsu Ueda[a,*]

[a] *Laboratory of Cellular Biochemistry, Division of Applied Life Sciences, Graduate School of Agriculture, Kyoto University, Kyoto 606-8502, Japan*
[b] *Department of Bio-Science, Faculty of Bio-Science, Nagahama Institute of Bio-Science and Technology, Shiga 526-0829, Japan*
[c] *Department of Physiology, Akita University School of Medicine, 1-1-1, Hondo, Akita 010-8543, Japan*

Received 31 August 2004
Available online 22 September 2004

Abstract

ABCA3 is highly expressed at the membrane of lamellar bodies in alveolar type II cells, in which pulmonary surfactant is stored. *ABCA3* gene mutations cause fatal surfactant deficiency in newborns. We established HEK293 cells stably expressing human ABCA3 and analyzed the function. Exogenously expressed ABCA3 is glycosylated and localized at the intracellular vesicle membrane. ABCA3 is efficiently photoaffinity labeled by 8-azido-[α^{32}P]ATP, but not by 8-azido-[γ^{32}P]ATP, when the membrane fraction is incubated in the presence of orthovanadate. Photoaffinity labeling of ABCA3 shows unique metal ion-dependence and is largely reduced by membrane pretreatment with 5% methyl-β-cyclodextrin, which depletes cholesterol. Electron micrographs show that HEK293/hABCA3 cells contain multivesicular, lamellar body-like structures, which do not exist in HEK293 host cells. Some fuzzy components such as lipids accumulate in the vesicles. These results suggest that ABCA3 shows ATPase activity, which is induced by lipids, and may be involved in the biogenesis of lamellar body-like structures.

Keywords: ABCA3; Cholesterol; Pulmonary surfactant; ATPase; ABC proteins; Lamellar body; Photoaffinity label

The lamellar body, in which pulmonary surfactant is stored, is a member of lysosome-related organelles also referred to as secretory lysosomes [1–3]. Lamellar bodies are secreted into the alveolar space by exocytosis. Secreted pulmonary surfactant coats the lumen of alveoli, where it reduces the surface tension at the alveolar air/liquid interface, thus preventing alveoli from collapsing and lowering the work of breathing. Pulmonary surfactant is composed of lipids (90%) and surfactant proteins (SP-A, SP-B, SP-C, and SP-D), which are densely packed into multilamellar structures. The most abundant lipid in pulmonary surfactant is phosphatidylcholine, especially dipalmitoylphosphatidylcholine. The mechanism by which lipids are packed into lamellar bodies is unknown.

The ATP-binding cassette transporter A3 (ABCA3) is predominantly expressed in lung [4,5] and localized to the limiting membrane of lamellar bodies in alveolar type II cells in humans and the rat [6,7]. Recently, it was revealed that *ABCA3* gene mutations cause fatal surfactant deficiency in newborns [8]. Some ABC transporters belonging to the ABCA subfamily are involved in the transmembrane transport of endogenous lipids such as ABCA1 [9], ABCA4 [10], and ABCA7 [11].

☆ *Abbreviations:* ABCA3, ATP-binding cassette transporter A3; MβCD, methyl-β-cyclodextrin; Endo H, Endoglycosidase H; PNGaseF, peptide *N*-glycosidase F; PBS, phosphate-buffered saline.

* Corresponding author. Fax: +81 75 753 6104.
E-mail address: uedak@kais.kyoto-u.ac.jp (K. Ueda).

0006-291X/$ - see front matter © 2004 Elsevier Inc. All rights reserved.
doi:10.1016/j.bbrc.2004.09.043

ABCA3 might function as a transmembrane transporter of lipid components found in pulmonary surfactant. The exclusive expression of ABCA3 in the limiting membrane of lamellar bodies further supports the hypothesis that ABCA3 is involved in the formation and/or secretion of pulmonary surfactant. However, the functions of ABCA3 are still unknown. In this study, the function of ABCA3 and its interaction with ATP were examined using HEK293 cells stably expressing human ABCA3 (hABCA3).

Materials and methods

Materials. Polyclonal antibody was raised against the C-terminal 13 amino acids of ABCA3. 8-Azido-[α^{32}P]ATP, 8-azido-[γ^{32}P]ATP, and 8-azido-[α^{32}P]ADP were purchased from Affinity Labeling Technologies. pcDNA3.1/*myc*-HisB and monoclonal antibody C219 were purchased from Invitrogen and Signet Laboratories, respectively. All other chemicals were obtained from Sigma, Wako Pure Chemical Industries, and Nacalai Tesque.

Transfection and establishment of HEK293 cells stably expressing hABCA3. HEK293 cells were cotransfected by pCMVhABCA3 and pcDNA3.1/*myc*-HisB with LipofectAMINE (Invitrogen) according to the manufacturer's instructions. Cells were selected by 1 mg/ml geneticin (G418) for 2 weeks. Single colonies were isolated, and the expression of hABCA3 was examined by Western blot analysis and immunofluorescent staining with anti-hABCA3 antibody. To establish HEK293 cell expressing human MDR1 (hMDR1), the cells were transfected with the hMDR1 expression vector pCAGGSP/MDR1 [12] and selected by 50–80 nM vinblastine for 2 weeks. Resistant cells were further selected by 400 nM vinblastine and 100 nM doxorubicin hydrochloride for 4 weeks. Mixed populations of vinblastine and doxorubicin resistant colonies were obtained, and the expression of hMDR1 was examined by Western blot analysis with monoclonal antibody C219.

Glycosylation of ABCA3. Endoglycosidase H (Endo H) and peptide *N*-glycosidase F (PNGaseF) (New England Biolabs, Beverly, MA) digestions were performed as described by the manufacturer. In brief, 20 μg of membrane proteins from HEK293 cells stably expressing ABCA3 was treated with 500 U Endo H or 0.3 U PNGaseF for 1 h at 37 °C. The deglycosylated proteins were separated by SDS–PAGE (7%) and analyzed by Western blot analysis by using anti-hABCA3 antibody.

Immunostaining and fluorescence microscopy. Cells were cultured on glass coverslips in Dulbecco's modified Eagle's medium supplemented with 10% (v/v) fetal bovine serum in 5% CO_2 at 37 °C. They were fixed with 4% paraformaldehyde and permeabilized with 0.4% Triton X-100 for 5 min. The cells and membranes were incubated overnight with anti-hABCA3 antibody, and then incubated with Alexa488-conjugated anti-rabbit IgG for 1 h. The cells and membranes were directly viewed with a 63× Plan-Neofluar or 100× Plan-Apochromat oil immersion objective using a Zeiss confocal microscope (LSM5 Pascal or LSM510).

Electron microscopy. HEK293 and HEK293/hABCA3 cells were cultured on plastic coverslips (Celldesk, LF1, Sumitomo Bakelite, Tokyo). For conventional electron microscopy, cells were fixed in 2.5% glutaraldehyde in 0.1 M cacodylate buffer (pH 7.4) for 3 h. The cells were washed in the same buffer three times and were post-fixed in 1% OsO_4 in the buffer for 1 h. After washing in distilled water, the cells were incubated with 50% ethanol for 10 min and block stained with 2% uranyl acetate in 70% ethanol for 2 h. They were further dehydrated with a graded series of ethanol and were embedded in epoxy resin. Ultra-thin sections were doubly stained with uranyl acetate and lead citrate, and observed under a Hitachi H7600 electron microscope (Hitachi, Tokyo, Japan).

Vanadate-induced nucleotide trapping in ABCA3 with 8-azido-[α^{32}P]ATP, 8-azido-[γ^{32}P]ATP or 8-azido-[α^{32}P]ADP. The membrane fraction was prepared by nitrogen cavitation as previously described [13]. The membrane fraction (15–30 μg) was incubated with 10 μM 8-azido-[α^{32}P]ATP, 2 mM ouabain, 0.1 mM EGTA, and 40 mM Tris–HCl (pH 7.5) in a total volume of 6–10 μl for 10 min at 37 °C in the presence or absence of 400 μM orthovanadate and 3 mM $MgSO_4$. The reaction was stopped by adding 400 μl ice-cold TE buffer (40 mM Tris–HCl (pH 7.5), 0.1 mM EGTA) containing 1 mM $MgSO_4$. The supernatant containing unbound ATP was removed from the membrane pellet after centrifugation (14.000 rpm, 5 min, 2 °C), and this procedure was repeated once more. The pellets were resuspended in 8 μl of TE buffer containing 1 mM $MgSO_4$ and irradiated for 1 min (254 nm, 8.2 mW/cm^2) on ice. The samples were then electrophoresed on a 7% SDS–polyacrylamide gel, transferred to a PVDF membrane, and analyzed by Western blotting. After antibody was removed, the PVDF membrane was further analyzed by autoradiography.

MβCD-pretreatment of the membrane fraction. The membrane fraction (30 μg) was incubated in 20 μl of 40 mM Tris buffer containing no or 5% (w/v) MβCD for 30 min at 25 °C. The supernatant was removed after centrifugation (14.000 rpm, 5 min, room temperature), and the pellets were washed with 40 mM Tris buffer and subjected to vanadate-induced nucleotide trapping.

Results

Stable expression of human ABCA3 in HEK293 cells

To study the function of human ABCA3, a cell line (HEK293/hABCA3) stably expressing hABCA3 was established. A crude membrane fraction was analyzed by Western blotting, and two bands at about 190 and 150 kDa were detected by using the anti-ABCA3 anti-

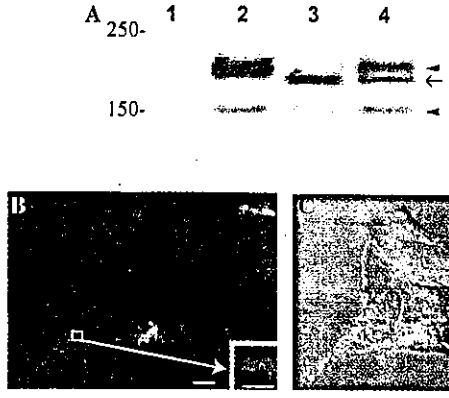

Fig. 1. (A) Western blot analysis and glycosylation of hABCA3 expressed in HEK293 cells. Membrane proteins (20 μg) prepared from HEK293 cells (lane 1) and HEK293/hABCA3 (lanes 2–4) were separated on 7% SDS–polyacrylamide gel. Membrane fractions were treated with PNGaseF (lane 3) or Endo H (lane 4), and Western blotting was done with anti-hABCA3 rabbit antibody. Immunoreactive bands of 190 and 150 kDa are indicated by the arrowheads. The deglycosylated 180 kDa ABCA3 is indicated by an arrow. (B) Immunofluorescence confocal microscopy analysis of HEK293/hABCA3 cells. Permeabilized cells were reacted with anti-hABCA3 antibody and anti-rabbit IgG-Alexa488. Scale bar, 5 μm. Inset: a magnified image of a part of the cell (marked by a square). Scale bar, 2 μm. (C) The overlaid image of ABCA3 fluorescence and differential interference contrast imaging.

body (Fig. 1A, lane 2, indicated by the arrowheads). No signal was detected in the membrane fraction prepared from HEK293 cells (Fig. 1A, lane 1). Glycosylation of ABCA3 was examined by the treatment with PNGaseF and Endo H. Endo H cleaves two proximal *N*-acetylglucosamine residues of the high mannose type but not of the complex type, while PNGaseF cleaves sugar chains of both types. Treatment with PNGaseF increased the electrophoretic mobility of 190 kDa ABCA3 to produce the 180 kDa protein (indicated by an arrow), which was the deglycosylated form. A large portion of the 190 kDa protein was insensitive to Endo H, but a portion of 190 kDa ABCA3 was sensitive to EndoH treatment resulting in the deglycosylated form. These results suggest that a large portion of ABCA3 contained complex-type sugar chains and was localized in the post-Golgi membrane. The 150 kDa protein was not affected by either glycosidase. Since the antibody was generated against the C-terminal 13 amino acids of hABCA3, the 150 kDa protein was not glycosylated and might have been a product of proteolytic cleavage at the N-terminus.

Subcellular localization of hABCA3 and the formation of vesicular structures in HEK293 cells

The subcellular localization of hABCA3 was analyzed by immunofluorescent confocal microscopy (Figs. 1B and C). ABCA3 was mainly localized at the intracellular vesicle membrane and showed a ring-like appearance (Fig. 1B, inset). Expression on the plasma membrane was rarely observed. ABCA3 immunoreactivity is mostly detected at the limiting membrane of lamellar bodies in the lung [6,7], and when EGFP-conjugated hABCA3 is expressed in human lung adenocarcinoma A549 cells, green fluorescence can be observed at the intracellular vesicle membrane [7]. The diameters of the vesicles observed in HEK293/hABCA3, at which ABCA3 was localized, were about 1 μm, corresponding with those of lamellar bodies.

Vanadate-induced nucleotide trapping in hABCA3

Next we examined if ABCA3 expressed in HEK293/hABCA3 cells was functional. Among the ABC proteins, MDR1 (ABCB1), MRP1 (ABCC1), and MRP2 (ABCC2), which transport various xenobiotics, efficiently trap Mg-ADP in the presence of orthovanadate, an analog of phosphate, and form a stable inhibitory intermediate during the ATP hydrolysis cycle. These intermediates can be specifically photoaffinity labeled in the membrane when 8-azido-[α^{32}P]ATP is used as an ATP analog [12,14–16]. For these proteins, vanadate-induced nucleotide trapping is stimulated by the addition of transport substrates, probably because they stimulate ATP hydrolysis.

To examine vanadate-induced nucleotide trapping in hABCA3, the membrane fraction was prepared from HEK293/hABCA3 cells, and observed by confocal microscopy after immunofluorescent staining to confirm the presence of ABCA3. ABCA3 immunoreactivity was detected in vesicular structures, suggesting that they were preserved during membrane preparation (Fig. 2A).

Proteins of 190 and 150 kDa were specifically photoaffinity-labeled among the membrane proteins from HEK293/hABCA3 when incubated with 8-azido-[α^{32}P]ATP in the presence of orthovanadate and Mg^{2+}, and were irradiated after removing free nucleotides (Fig. 2B, the upper panel, lane 1). These labeled proteins were identified as ABCA3 by Western blot analysis (Fig. 2B, the lower panel). hABCA3 was only weakly photoaffinity-labeled in the absence of orthovanadate, and no protein was labeled in HEK293 host cells (data not shown). These results suggested that a stable inhibitory intermediate of ABCA3 was formed with orthovanadate during the ATP hydrolysis cycle.

To confirm that the photoaffinity-labeled ABCA3 trapped ADP after hydrolysis, the same experiment was performed using 8-azido-[γ^{32}P]ATP (Fig. 2B, lanes 3 and 4). ABCA3 was weakly photoaffinity-labeled by 8-azido-[γ^{32}P]ATP in the absence of orthovanadate. However, the photoaffinity-labeling was not enhanced by the addition of orthovanadate. When 8-azido-[α^{32}P]ADP was used as an ATP analog, hABCA3 was also photoaffinity-labeled in an orthovanadate-dependent manner (shown later in Fig. 3C). These results suggested that the stable inhibitory complex ABCA·3MgADP·Vi was formed in the membrane fraction after ATP hydrolysis, as was the case with transporter-type ABC proteins.

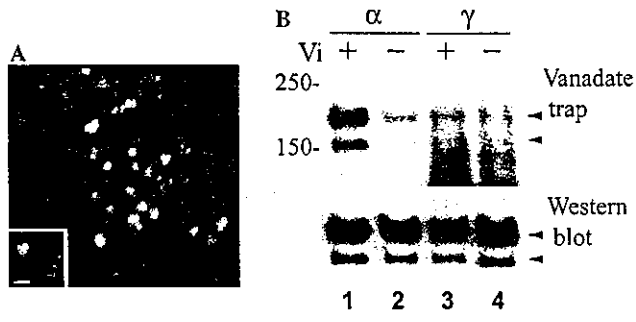

Fig. 2. Vanadate-induced nucleotide trapping (vanadate trap) in hABCA3. (A) An immunofluorescent confocal micrograph of crude membrane fraction prepared from HEK293/hABCA3. Inset, a magnified image. Scale bar, 1 μm. (B) Upper panel: vanadate trap with 8-azido-[α^{32}P]ATP or 8-azido-[γ^{32}P]ATP. Membranes (20 μg) were incubated with 10 μM 8-azido-[α^{32}P]ATP (α) or 8-azido-[γ^{32}P]ATP (γ) in the presence (+) or absence (−) of 400 μM orthovanadate at 37 °C for 10 min. Lower panel: Western blot analysis of the blot used for vanadate trap with anti-hABCA3 antibody. hABCA3 bands are indicated by the arrowheads.

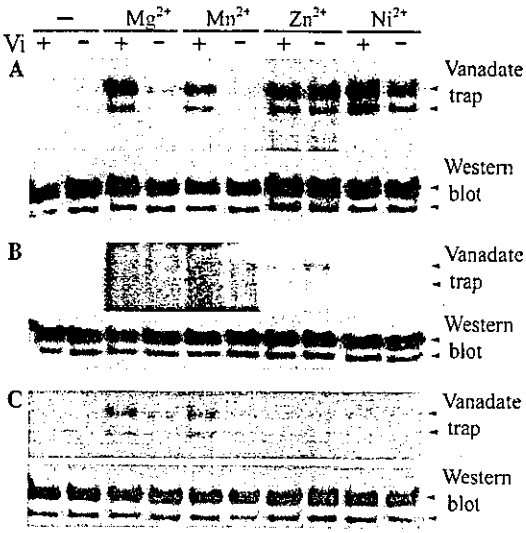

Fig. 3. Effect of metal ions on photoaffinity labeling by 8-azido-[α^{32}P]ATP (A), 8-azido-[γ^{32}P]ATP (B) or 8-azido-[α^{32}P]ADP (C). Upper panels (vanadate trap): membranes were incubated with 10 μM 8-azido-[α^{32}P]ATP (A), 8-azido-[γ^{32}P]ATP (B) or 8-azido-[α^{32}P]ADP (C), and 3 mM $MgSO_4$, $MnCl_2$, $ZnCl_2$, or $NiCl_2$, in the presence (+) or absence (–) of 400 μM orthovanadate at 37 °C for 10 min. Lower panels: Western blot analysis of the blot used for vanadate trap with anti-hABCA3 antibody. hABCA3 bands are indicated by the arrowheads.

Effect of metal ions on vanadate-induced nucleotide trapping in hABCA3

The divalent cation dependence of vanadate-induced nucleotide trapping varies among ABC proteins. Although trapping occurs with Mg^{2+}, Mn^{2+} or other divalent cations in MDR1 and MRP1, it occurs in the presence of Ni^{2+} but not Mg^{2+} in MRP6 (ABCC6) [17]. We examined the dependence of ABCA3 photoaffinity labeling on the divalent cations Mg^{2+}, Mn^{2+}, Zn^{2+}, and Ni^{2+} (Fig. 3A).

In the presence of Mn^{2+}, ABCA3 was photoaffinity-labeled in a vanadate-dependent manner as occurred in the presence of Mg^{2+}, but the efficiency was lower. In the presence of Zn^{2+}, ABCA3 was photoaffinity-labeled as strongly as in the presence of Mg^{2+}. However, labeling in the presence of Zn^{2+} was not dependent on orthovanadate. Labeling in the presence of Ni^{2+} was stronger than in the presence of Mg^{2+}. In addition, labeling occurred even in the absence of orthovanadate.

Since efficient photoaffinity-labeling was observed even in the absence of orthovanadate using Zn^{2+} and Ni^{2+}, we examined whether labeling occurs after hydrolysis. When the reaction was carried out using 8-azido-[γ^{32}P]ATP, ABCA3 was rarely photoaffinity-labeled, suggesting that 8-azido-[γ^{32}P]ATP was hydrolyzed and γ-phosphate was released (Fig. 3B). However, it was also rarely photoaffinity-labeled with 8-azido-[α^{32}P]ADP in the presence of Zn^{2+} and Ni^{2+} (Fig. 3C), although photoaffinity labeling was observed in the presence of Mg^{2+} and Mn^{2+}. These results suggest that the stable complexes ABCA3ZnADP and ABCA3NiADP formed only during ATP hydrolysis.

MβCD-pretreatment suppressed nucleotide trapping in hABCA3

Since efficient vanadate-induced nucleotide trapping in ABCA3 was observed without exogenously added substrates, we speculated that endogenous substrate(s) of ABCA3 were present in the membrane fraction. Lipids and surfactant proteins are densely packed in lamellar bodies, and therefore phospholipids and/or cholesterol are likely to be substrates of ABCA3. To examine the validity of this hypothesis, the membrane fraction was treated with 5% MβCD, which depletes cholesterol from the membrane [18–20], at 25 °C for 30 min before reaction with 8-azido-[α^{32}P]ATP. Vanadate-induced nucleotide trapping in hABCA3 was strongly suppressed by the treatment with 5% MβCD (Fig. 4A).

We also examined the effect of MβCD-pretreatment on vanadate-induced nucleotide trapping in MDR1, whose endogenous substrate was suggested to be cholesterol [21]. Vanadate-induced nucleotide trapping in MDR1 in the absence of exogenously added substrate was suppressed by treatment with 5% MβCD (Fig. 4B). In the presence of verapamil, a transport substrate of MDR1, photoaffinity labeling occurred efficiently, even after treatment with 5% MβCD (Fig. 4B). These results suggest that substrate recognition and ATP hydrolysis by MDR1 are not impaired by treatment with 5% MβCD. Therefore, reduced vanadate-induced nucleotide trapping in ABCA3 and MDR1 by treatment with 5% MβCD was due to the depletion of endogenous substrates, most likely cholesterol, from the membrane.

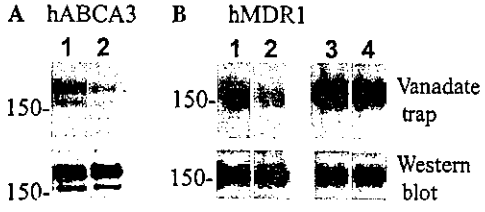

Fig. 4. Effect of MβCD treatment on vanadate-induced nucleotide trapping in hABCA3 and hMDR1. (A) Membranes prepared from HEK293/hABCA3 pretreated without (lane 1) or with 5% MβCD (lane 2) at 25 °C for 30 min. Upper panel: vanadate trap with 10 μM 8-azido-[α^{32}P]ATP at 37 °C for 10 min. Lower panel: Western blot analysis of the blot used for vanadate trap with anti-hABCA3 antibody. (B) Membranes prepared from HEK293/hMDR1 pretreated without (lanes 1 and 3) or with 5% MβCD (lanes 2 and 4) at 25 °C for 30 min. Upper panels: vanadate trap with 10 μM of 8-azido-[α^{32}P]ATP in the absence (lanes 1 and 2) or presence (lanes 3 and 4) of 25 μM verapamil at 37 °C for 10 min. Lower panels: Western blot analysis of the blot used for vanadate trap with anti-MDR1 antibody C219.

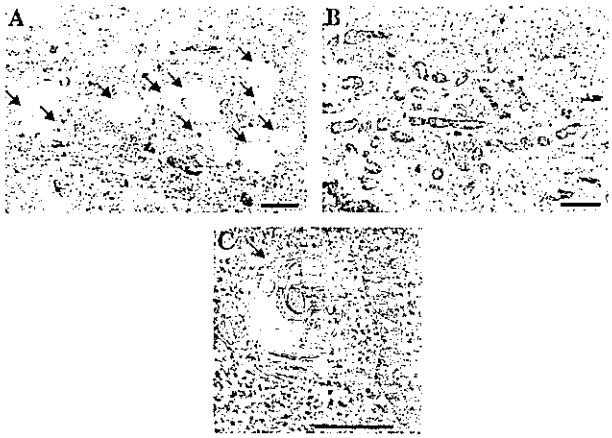

Fig. 5. Electron micrograph of HEK293/hABCA3 (A,C) and HEK293 host cells (B). Lamellar body-like structures are indicated by the arrows. Scale bars, 1 μm.

Generation of lamellar body-like structures in HEK293/hABCA3

Finally, HEK293/hABCA3 cells were observed by electron microscopy and compared with HEK293 host cells to confirm that the vesicular structures were generated by exogenously expressed ABCA3. In HEK293/hABCA3 cells, many unique vesicles 0.6–1 μm in diameter were observed (Figs. 5A and C). They appeared to be multilamellar and contained fuzzy components. These lamellar vesicular structures were scarcely observed in HEK293 host cells (Fig. 5B).

Discussion

Because *ABCA3* gene mutations cause fatal surfactant deficiency in newborns [8], the function of ABCA3 is crucial for the formation and/or secretion of pulmonary surfactant. However, the function of ABCA3 is still unknown. In this study, we showed that exogenously expressed ABCA3 generates vesicular structures in HEK293 cells. Electron micrographs show that HEK293/hABCA3 cells contain multivesicular, lamellar body-like structures, which do not exist in HEK293 host cells. Some fuzzy components such as lipids accumulate in the vesicles. These results suggest that ABCA3 may be involved in the generation of lamellar body-like structures.

ABCA3 is strongly photoaffinity labeled by 8-azido-[α^{32}P]ATP when the membrane fraction is incubated in the presence of Mg^{2+} and orthovanadate. Photoaffinity labeling by 8-azido-[γ^{32}P]ATP is weak and is not stimulated by the addition of orthovanadate, indicating that ABCA3 shows strong ATPase activity in the isolated membrane. Vanadate-induced nucleotide trapping in ABCA3 was strongly suppressed by pretreatment of the membrane with MβCD, which depletes cholesterol [18–20]. The basal vanadate-induced nucleotide trapping in MDR1, whose endogenous substrate is suggested to be cholesterol [21], is also inhibited by pretreatment of the membrane with MβCD. The reduction of photoaffinity labeling of ABCA3 and MDR1 is most likely due to cholesterol depletion from the membrane. These results suggest that cholesterol may be a transport substrate for ABCA3. Alternatively, MβCD might deplete phospholipids together with cholesterol. Because dipalmitoylphosphatidylcholine, most abundant lipid in pulmonary surfactant, has high affinity to cholesterol, it is possible that phospholipids with saturated fatty acid chains are also depleted from HEK293 cell membrane together with cholesterol. This might cause the suppression of vanadate-induced nucleotide trapping in ABCA3.

The dependence of photoaffinity labeling of ABCA3 on divalent cations showed a specific and unusual pattern. The most striking feature of ABCA3 was the strong photoaffinity labeling in the presence of Zn^{2+} and Ni^{2+}, which was not dependent on orthovanadate. Since ABCA3 was scarcely photoaffinity labeled by 8-azido-[γ^{32}P]ATP, 8-azido-ATP was hydrolyzed and γ-phosphate was released before a stable complex was formed. The state of the inhibitory complex was further examined using 8-azido-[α^{32}P]ADP. ABCA3 was photoaffinity labeled by 8-azido-[α^{32}P]ADP in the presence of Mg^{2+} and Mn^{2+} in a vanadate-dependent manner. However, it rarely occurred in the presence of Zn^{2+} or Ni^{2+}. These results suggest that a stable ABCA3·MeADP·Vi complex, where Me is Mg^{2+} or Mn^{2+}, can be formed in two ways. In one way, it is formed after ATP hydrolysis in the presence of orthovanadate, and in the other way ADP takes part in the stable ABCA3·MeADP·Vi complex without ATP hydrolysis. In contrast, in the presence of Zn^{2+} and Ni^{2+}, stable complexes form even without vanadate, and ADP cannot take part in the complex without ATP hydrolysis. Conformational changes caused by ATP hydrolysis are likely required to form this stable complex. The relevance of this phenomenon to the physiological role of ABCA3 remains to be solved.

hABCA3 was detected as 190 and 150 kDa proteins by immunoblot analysis using antibody generated against the C-terminal 13 amino acids of hABCA3 when stably expressed in HEK293 cells. It was previously reported that hABCA3 was detected as a single band 150-kDa protein in the crude membrane fraction of human lung tissue using the same antibody [6]. This can be explained by the cleavage of hABCA3 at its N-terminus, producing the mature form of the 150-kDa protein. The 150-kDa protein in HEK293/hABCA3 might also be a product of proteolytic cleavage. There are two consensus amino acid sequences (asparadine-124 and asparadine-140), which can be modified by N-linked oligosaccharides, in the first extracytosolic domain.